Zoosyst. Evol. 97 (1) 2021, 249–272 | DOI 10.3897/zse.97.61351

PENSOFT

MUSEUM FÜR NATURKUNDE BERLIN

Lizards of a different stripe: phylogenetics of the *Pedioplanis undata* species complex (Squamata, Lacertidae), with the description of two new species

Jackie L. Childers[1], Sebastian Kirchhof[2,3], Aaron M. Bauer[4]

1 *Museum of Vertebrate Zoology, University of California, Berkeley, California 94720, USA*

2 *Museum für Naturkunde, Leibniz Institute for Evolution and Biodiversity Science, Invalidenstr. 43, 10115 Berlin, Germany*

3 *New York University Abu Dhabi, Saadiyat Island, Abu Dhabi, United Arab Emirates*

4 *Department of Biology and Center for Biodiversity and Ecosystem Stewardship, Villanova University, 800 Lancaster Avenue, Villanova, Pennsylvania 19085, USA*

http://zoobank.org/892D728A-F413-4E83-A808-575EA1A3D320

Corresponding author: Jackie L. Childers (jchilders@berkeley.edu)

Academic editor: Johannes Penner ♦ **Received** 25 November 2020 ♦ **Accepted** 22 March 2021 ♦ **Published** 23 April 2021

Abstract

The lacertid genus *Pedioplanis* is a moderately speciose group of small-bodied, cryptically-colored lizards found in arid habitats throughout southern Africa. Previous phylogenetic work on *Pedioplanis* has determined its placement within the broader context of the Lacertidae, but interspecific relations within the genus remain unsettled, particularly within the *P. undata* species complex, a group largely endemic to Namibia. We greatly expanded taxon sampling for members of the *P. undata* complex and other *Pedioplanis*, and generated molecular sequence data from 1,937 bp of mtDNA (ND2 and cyt *b*) and 2,015 bp of nDNA (KIF24, PRLR, RAG-1) which were combined with sequences from GenBank resulting in a final dataset of 455 individuals. Both maximum likelihood and Bayesian analyses recover similar phylogenetic results and reveal the polyphyly of *P. undata* and *P. inornata* as presently construed. We confirm that *P. husabensis* is sister to the group comprising the *P. undata* complex plus the Angolan sister species *P. huntleyi* + *P. haackei* and demonstrate that *P. benguelensis* lies outside of this clade in its entirety. The complex itself comprises six species including *P. undata*, *P. inornata*, *P. rubens*, *P. gaerdesi* and two previously undescribed entities. Based on divergence date estimates, the *P. undata* species complex began diversifying in the late Miocene (5.3 ± 1.6 MYA) with the most recent cladogenetic events dating to the Pliocene (2.6 ± 1.0 MYA), making this assemblage relatively young compared to the genus *Pedioplanis* as a whole, the origin of which dates back to the mid-Miocene (13.5 ± 1.8 MYA). Using an integrative approach, we here describe *Pedioplanis branchi* **sp. nov.** and *Pedioplanis mayeri* **sp. nov.** representing northern populations previously assigned to *P. inornata* and *P. undata*, respectively. These entities were first flagged as possible new species by Berger-Dell'mour and Mayer over thirty years ago but were never formally described. The new species are supported chiefly by differences in coloration and by unique amino acid substitutions. We provide comprehensive maps depicting historical records based on museum specimens plus new records from this study for all members of the *P. undata* complex and *P. husabensis*. We suggest that climatic oscillations of the Upper Miocene and Pliocene-Pleistocene era in concert with the formation of biogeographic barriers have led to population isolation, gene flow restrictions and ultimately cladogenesis in the *P. undata* complex.

Key Words

Biogeography, molecular phylogeny, phylogenetics, southern Africa, species description, taxonomy

Introduction

The Lacertidae is a large family of Old World lizards with a center of diversity in southern Africa, particularly in xerothermic habitats (Arnold et al. 2007; Mayer and Pavlicev 2007; Garcia-Porta et al. 2019). Overall, this family has a conservative general morphology and the degree of homoplasy and convergence in external features is very high, especially in predominantly arid-zone lineages (Borsuk-Bialynicka et al. 1999; Hipsley and Müller 2017). With 13 currently recognized species, *Pedioplanis* Fitzinger, 1843 is the most diverse genus of lacertid lizards in southern Africa (Conradie et al. 2012), with taxa occupying semi-arid to highly xeric habitats, including coastal fynbos, Nama and succulent Karoo, grassland, savannah, and hard-packed gravel plains and deserts (Branch 1998; Makokha et al. 2007). Nevertheless, previous studies have detected additional, novel lineages among *Pedioplanis* species that await resolution and formal description (Mayer and Berger-Dell'mour 1987; Makokha et al. 2007; Conradie et al. 2012). Members of the *Pedioplanis undata* species complex are autochthonous to Namibia and South Africa and have proven particularly taxonomically challenging (Mayer and Berger-Dell'mour 1987; Makokha et al. 2007). All are similar in size (adult SVL 40–56 mm) and overall body form, but exhibit differences in dorsal patterning and coloration, arrangement of scales in the lower eyelid, and geographic distribution (Mayer and Berger-Dell'mour 1987; Branch 1998; Makokha et al. 2007).

Pedioplanis undata was originally described as a single widespread species, *Lacerta undata* Smith, 1838, and one year later transferred to the genus *Eremias* Fitzinger, 1834 by Duméril and Bibron (1839). Three non-nominotypical subspecies, *Eremias undata rubens*, *E. u. gaerdesi* and *E. u. inornata* (the last originally described as full species, *Eremias inornata* Roux, 1907) were subsequently recognized based on morphological differences (Boulenger 1921; Mertens 1954, 1955). Mayer and Berger-Dell'mour (1987) used allozyme data to delineate a total of seven geographically coherent forms including northern and southern varieties of *P. u. undata* and *P. u. inornata*. They provisionally elevated *P. gaerdesi* and *P. rubens* to full species, and later used the same methods to describe *P. husabensis*, which together with *P. u. undata* and *P. u. inornata* resulted in five putative members of the complex (Berger-Dell'mour and Mayer 1989). Morphologically-based phylogenetic analyses by Arnold (1991) recovered the same five named taxa at the species level, although their results suggested that the *P. undata* complex was rendered paraphyletic by *P. namaquensis* and *P. benguelensis*.

Multiple recent molecular phylogenies have confirmed the monophyly of the *P. undata* species complex (including *P. husabensis*, as sister to all remaining species; Makokha et al. 2007; Conradie et al. 2012), however, some interspecific relationships remain unresolved. Maximum likelihood analyses place *P. rubens* in a clade with *P. undata* that is sister to all remaining species within the complex (Makokha et al. 2007), whereas Bayesian analyses suggest that the former is more deeply nested within the complex (Makokha et al. 2007; Conradie et al. 2012). The monophyly of *P. inornata* has also been an ongoing subject of debate. Makokha et al. (2007) identified two moderately divergent (ND2 = 7–8%; 16S rRNA = 3–4%; RAG-1 = 1–2%) lineages within the species, a west-central Namibian clade and a southern Namibian/Northern Cape (South Africa) clade. *Pedioplanis gaerdesi* was recovered as the sister to the former, rendering *P. inornata* paraphyletic (Makokha et al. 2007). These results corroborate Mayer and Berger-Dell'mour's (1987) report of two morphologically and geographically distinct forms of *P. inornata*, however, no formal taxonomic changes were made due to limited geographic sampling. Finally, the status of *P. undata* has also previously come into question, as Mayer and Berger-Dell'mour (1987) identified northern and southern forms of the species, yet the most recent phylogenetic analyses detected no such divergent clades given their limited sampling (Makokha et al. 2007; Conradie et al. 2012).

We present the most comprehensive phylogenetic assessment yet of the *P. undata* species complex in order to resolve interspecific relationships among described species, investigate the status of previously recognized unnamed lineages, and elucidate the geography of species diversification within the complex. We compiled a new and extended multi-locus dataset and reconstructed the phylogeny of the genus *Pedioplanis* as a whole with a greatly increased sample set for each member of the *P. undata* species complex throughout their ranges, particularly in Namibia.

Materials and methods

Field sampling

The majority of specimens included in this study were collected by the authors, under permitted fieldwork in Namibia, South Africa and Botswana. Specimens were euthanized, fixed in 10% neutral buffered formalin, and stored in 70–75% ethanol (EtOH). Prior to fixation, tail, thigh muscle or liver tissue was preserved in 95% EtOH for subsequent DNA sequencing. Specimens have been deposited in the Museum of Comparative Zoology at Harvard University (MCZ), the California Academy of Sciences (CAS), the National Museum of Namibia in Windhoek (NMNW), and the Museum für Naturkunde in Berlin (MfN, ZMB). All locality data were recorded by means of handheld GPS devices in decimal degrees (DD) using the WGS 84 reference coordinate system.

Molecular phylogeny

Genomic DNA was extracted using the Qiagen DNAeasy Kit. PCR amplification was performed on an Eppendorf Mastercycler gradient thermocycler using primer pairs

obtained from published sources (see Suppl. material 4: Table S1 for primer pairs). Molecular sequence data were generated for two mitochondrial genes, *NADH dehydrogenase subunit 2* (ND2) and *cytochrome b* (cyt *b*), and for three nuclear genes, *recombination activation gene 1* (RAG-1), *prolactin receptor* (PRLR), and *kinesin family member 24* (KIF24). Nuclear genes were sequenced for only a subsample of individuals representing unique mitochondrial haplotypes (KIF24: n = 229; PRLR: n = 214; RAG-1: n = 244). PCR products were visualized using 1.5% agarose gels and then purified with a homemade magnetic bead solution (Rohland and Reich 2012). Cycle Sequencing was performed using the BigDye Terminator v3.1 Cycle Sequencing Kit (Applied Biosystems, Foster City, CA, USA) and purified with an additional magnetic bead cleanup before being sequenced on an ABI 3730xl DNA analyzer. Sequences were assembled and edited in Geneious v9.1.8; initial sequence alignments were made using MUSCLE v3.8.31 (Edgar 2004) before adjusting by eye. Sequence alignments were used to calculate average uncorrected pairwise genetic distances (p-distance) using the distance matrices generated in Geneious v9.1.8.

Sequences were generated for 428 individuals, including all 13 currently recognized species of *Pedioplanis* and eight outgroup taxa (*Nucras aurantiacus*, *N. holubi*, *N. tessellata*, *Heliobolus lugubris*, *Ichnotropis capensis*, *Meroles knoxii*, *M. reticulatus*, *M. suborbitalis*). Based on recent molecular phylogenies (Mayer and Pavlicev 2007; Engleder et al. 2013) the sister pair *Nucras* + *Heliobolus* were used to root the tree. Within the *P. undata* species complex, the number of individuals for which sequences were generated are as follows: 18 *P. husabensis* (14 localities, see Kirchhof et al. 2017), 71 *P. undata* (28 localities), three *P. rubens* (2 localities), 110 *P. inornata* (58 localities), 48 *P. gaerdesi* (37 localities). Additional *Pedioplanis* sequences from the genes ND2 (n = 45) and RAG-1 (n = 40) were downloaded from GenBank, providing thorough representation of each species across its known geographic range (see Suppl. material 1 for complete list of tissue specimen and GenBank sampling).

Phylogenetic analyses using Maximum likelihood (ML) and Bayesian inference (BI) were performed on the CIPRES Science Gateway v3.3 (Miller et al. 2010). Separate analyses were performed on individual genes and on the concatenated sets of mitochondrial and nuclear genes separately. Best-fitting models of evolution were identified using PartitionFinder v.2.1.1 (Lanfear et al. 2016) in which partitioning schemes were selected using the Bayesian Information Criterion (BIC) score for each analysis. All ML partitions were run under the GTR+Γ model of evolution using RAxML v8.1.24 (Stamatakis 2014) for 1,000 rapid nonparametric bootstrap replicates; BI partitions were run under the models listed in Suppl. material 5: Table S2. MrBayes v3.2.6 (Ronquist and Huelsenbeck 2003) was used to perform all Bayesian phylogenetic analyses and run for 50,000,000 generations, sampling every 10,000 generations; convergence of the Markov chains was assessed by eye using Tracer v1.7 (Rambaut et al. 2018) and the initial 25% of trees were discarded as burn-in.

Morphological data and analysis

Morphological comparisons among members of the *P. undata* complex were made following initial phylogenetic analysis. A diversity of mensural and meristic measures was recorded for 120 specimens including the type series of the new species described herein, and additional specimens representative of major clades revealed by the phylogenetic analyses. In order to obtain adequate sampling to capture morphological variation in each clade, we added non-genotyped adult individuals (≥ 40 mm snout–vent length) of *P. undata* sensu stricto (n = 6) collected from the Oanob Dam (near Rehoboth) population, and of *P. rubens* (n = 9) from the Klein Waterberg population, to the morphological analyses (see Appendix 1 for a complete list of specimens used for the morphological analyses). Morphological data included the following measurements in mm (for bilateral features only right side values were recorded, unless damaged): Snout–vent length (SVL) – snout tip to the anterior edge of the cloaca; body length (BL) – anterior edge of cloaca to posterior edge of collar; collar-snout length (CSL) – posterior edge of collar to snout tip; head length (HL) – posterior edge of the occipital to snout tip; maximum head width (HW); lower jaw length (JL) – anterior edge of jaw bone to tip of lower jaw; length of the fourth finger (FiL) and fourth toe (ToL); inter-limb length (IL)– length between axillary and inguinal regions; hind limb (tibia) length (HiL); forearm length (FoL) – elbow to wrist; tail length (TaL) – posterior edge of cloaca to tail tip. All measurements were collected using Mitutoyo digital calipers (to 0.1 mm). Comparative data for Angolan taxa were obtained from Conradie et al. (2012).

Features of head and body scalation recorded were: prefrontal contact (PF); number of small granules in front of supraoculars touching frontal and prefrontal (G); number of rows of granules between supraoculars and supraciliaries (RG); number of supraciliaries (Su); interparietal-occipital contact (IO); number of infralabials (IF); number of gular scales in a straight line between the chin symphysis and median collar plate (Gu); number of subdigital lamellae on fourth toe (SuL); number of femoral pores on right leg (left if right leg was damaged or pores obscured) (Fe). Features of dorsal color and pattern were also recorded. All recorded morphological data for the type specimens are reported in the species descriptions below and listed in Tables 1 and 2; summaries of the meristic and mensural character data for members of the *P. undata* species complex can be found in Suppl. materials 2, 3 (Suppl. material 2: mensural character data for *P. undata* species complex voucher specimens; Suppl. material 3: meristic character data for *P. undata* species complex voucher specimens).

X-rays and Micro-computed (micro-CT) scans of specimens in the type series designated in this study were prepared at the California Academy of Sciences and Museum für Naturkunde, respectively, to obtain presacral vertebrae counts (PV). All x-ray images were taken using a Faxitron Cabinet X-ray System Model 43855C (Faxitron, Tucson, AZ, USA) at 45 kV for 60 s. Micro-CT scans were obtained using a Phoenix nanotom X-ray|s tube at 85 kV and 120 or 150 µA, generating 1440 projections with 750 ms per scan, with differing kV-settings depending on the respective specimen size. Effective voxel size, i.e., resolution in three-dimensional space, ranged from 12.8 to 14.3 µm. The cone beam reconstruction was performed using the datos|x-reconstruction software (GE Sensing & Inspection Technologies GMBH phoenix|x-ray datos|x 2.2) and the data were visualized in VG Studio Max 3.1. Micro-CT scans have been deposited on the MfN data repository (https://doi.naturkundemuseum.berlin/10.7479/4jg6-ae46) and are available on the MorphoSource website (http://morphosource.org). X-ray images are also available on MorphoSource (See Appendix 1 for DOIs).

Due to limited sample sizes we ran our morphological analyses on a dataset combining data for adult males and females of each species; all statistical analyses were performed in R (R Core Team 2019). Meristic variables were tested for normal distribution using the Shapiro-Wilk normality test as part of the R package dplyr (Wickham et al. 2021) and for homogeneity of variance with Levene's test using the package car (Fox and Weisberg 2019). They were then compared between species using one-way ANOVA (for normally distributed data with homogeneity of variance) or Kruskal-Wallis rank sum test (for skewed data or data without homogeneity of variance). We excluded the categorical variables prefrontal contact (PF) and interparietal-occipital contact (IO) and number of rows of granules between supraoculars and supraciliaries (RG) from this analysis.

Allometric effects were taken into account when mensural characters were compared. We built bivariate linear models using the raw measurements of each character in relation to the respective individual's SVL and compared the slopes of the regression lines visually using the ggplot2 package (Wickham 2016). We refrained from additional multivariate analyses due to a concern that doing so would potentially lead to unreliable results as a consequence of comparatively smaller sample sizes in the datasets.

Results

Phylogenetic analysis

Final alignments of the in-group *Pedioplanis* taxa were as follows: ND2: 905 base pairs (429 variable, 379 parsimony informative); cyt *b*: 1,032 base pairs (444 variable, 363 parsimony informative); KIF24: 484 base pairs (72 variable, 50 parsimony informative); PRLR: 544 base pairs (73 variable, 46 parsimony informative); RAG-1: 987 base pairs (124 variable, 74 parsimony informative).

There were no conflicts in the topologies between the BI and ML analyses and both retrieved generally high nodal support (bootstraps – BS > 70%; posterior probabilities – PP > 0.95) throughout their respective trees. Separate analyses among the nuclear genes revealed no conflicts, though individually they provided little resolution and were thus concatenated into a single alignment. Within the concatenated nuclear tree (not shown) *P. benguelensis*, *P. husabensis* and *P. rubens* were found to be monophyletic with strong support (*P. benguelensis*: PP = 1.0, BS = 100%; *P. husabensis*: PP = 1.0, BS = 100%; *P. rubens*: PP = 0.85, BS = 100%). However, all supraspecific clades within the *P. undata* complex were weakly supported by our nuclear data, and relationships among them remained largely unresolved.

Separate analyses were performed on the individual and concatenated mitochondrial genes ND2 and cyt *b*. Each analysis resulted in a well-resolved tree and no taxonomically relevant topological conflicts were revealed. Our concatenated mitochondrial analyses (Fig. 1) recovered a strongly supported monophyletic *Pedioplanis* as sister to *Meroles* + *Ichnotropis* (PP = 1.0, BS = 98%). Within *Pedioplanis*, *P. burchelli* + *P. laticeps* are sister to all remaining congeners (PP = 1.0, BS = 100%). *Pedioplanis breviceps* and *P. lineoocellata* are recovered as sister taxa (PP = 1.0, BS = 100%) and are, in turn, sister to *P. namaquensis* plus all remaining *Pedioplanis* (PP = 1.0, BS = 100%). *Pedioplanis benguelensis*, *P. husabensis* and (*P. huntleyi* + *P. haackei*) are successively more closely related to the *P. undata* complex (PP = 1.0, BS = 99–100%).

Within the clade containing the four recognized species of the *P. undata* species complex (*P. undata*, *P. gaerdesi*, *P. inornata*, *P. rubens*) we recovered a total of six highly divergent lineages (Figs 1, 2). In all analyses *P. undata* appears polyphyletic, comprising two geographically distinct lineages, one from northern Namibia (*P. undata* "North" sensu Mayer and Berger-Dell'mour 1987) and another that occurs in central Namibia from the Khomas Highlands, south into parts of the northern Hardap Region and west into the Erongo Region (*P. undata* "South" sensu Mayer and Berger-Dell'mour 1987). The two forms were not recovered as sister taxa and are highly divergent from one another (average uncorrected p-distance + SD: cyt *b*: 12% + 0.9; ND2: 14% + 4.1). The southern lineage is deeply nested within the complex, whereas *P. undata* "North" is sister to all other *P. undata* complex lineages (PP = 1.0, BS = 100%). *Pedioplanis rubens* was recovered nested within the *P. undata* species complex and sister to the remaining clades (PP = 1.0, BS = 99%). Individuals that superficially resemble *P. inornata* or *P. gaerdesi* from central-west Namibia in the Erongo region form a clade, (*P. inornata* "Central" sensu Makokha et al. 2007) and are sister to *P. gaerdesi* sensu stricto (PP = 1.0, BS = 100%), collected largely from north of the Ugab River. A second *P. inornata* clade (*P. inornata* "South") was represented by specimens from as far north as the Kuiseb River and south into the Northern Cape Province of South Africa. These *P. inornata* lineages are moderately divergent

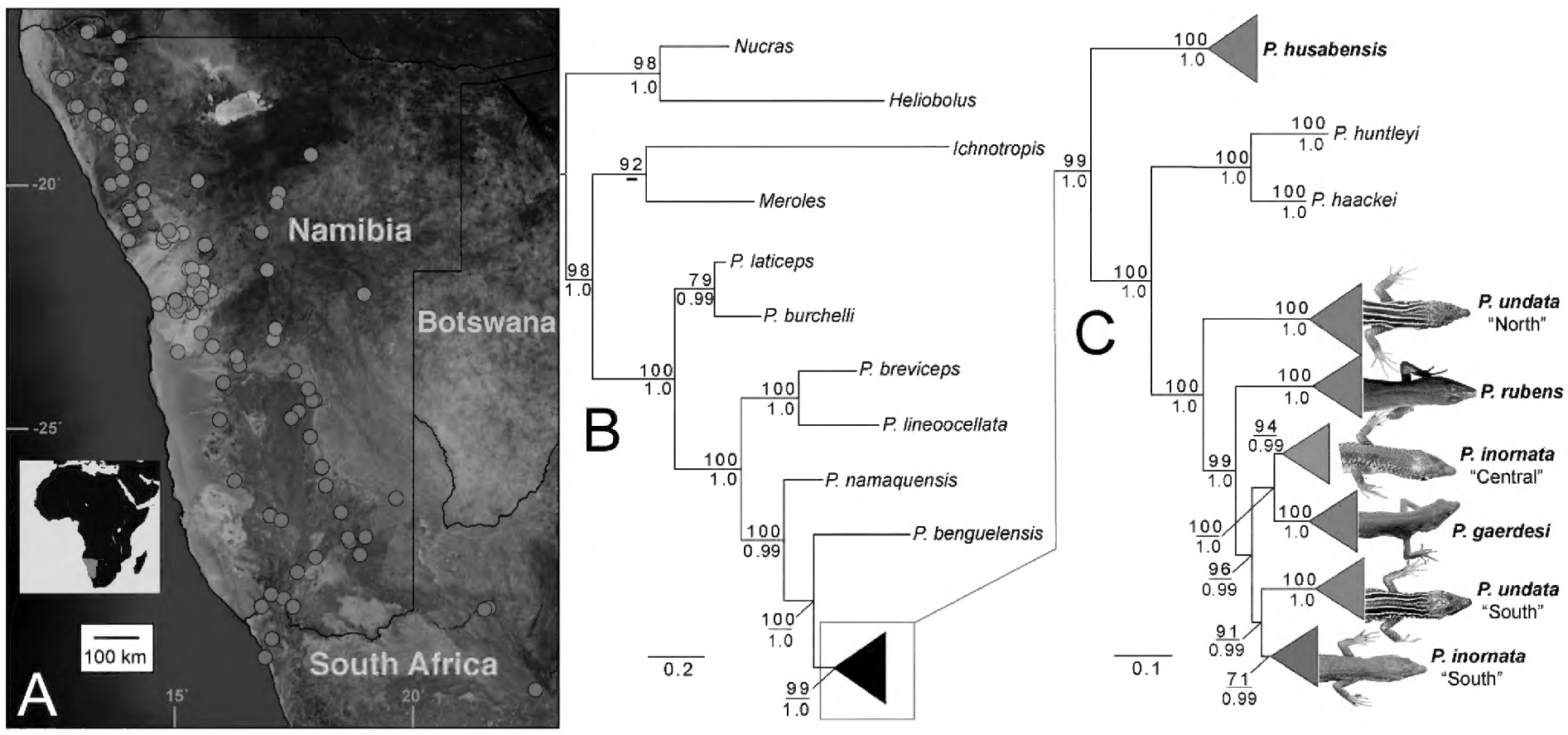

Figure 1. Sampling map and phylogeny of *Pedioplanis*. (**a.**) Satellite map of Namibia depicting sampling localities for genotyped specimens of *P. husabensis* and the six major clades within the *P. undata* species complex recovered by maximum likelihood and Bayesian analysis of the concatenated mitochondrial dataset. (**b**, **c.**) Maximum likelihood phylogram depicting (**b.**) the interspecific phylogenetic relationships among all *Pedioplanis* species and (**c.**) all major clades within the *P. undata* species complex; colored triangles indicate multiple sequenced individuals; typical dorsal patterning for each member of the complex is shown based on photographs of live individuals and museum vouchers. Bootstrap values (above) and posterior probabilities (below) are provided for each major node. Satellite map of Namibia and surrounding countries created by using the Google Maps terrain map layer, which was accessed through the Free and Open Source QGIS (QGIS.org 2021) and its OpenLayers Plugin.

from each other (average uncorrected p-distance + SD): cyt *b*: 7.7% + 0.5; ND2: 8.8% + 4.3). A sister relationship between *P. undata* "South" and *P. inornata* "South" is recovered in all analyses (PP = 0.99, BS = 91%), although without support in the case of nuclear data. A sampling map for sequenced tissues of *P. husabensis* and all clades recovered within the *P. undata* species complex is depicted in Fig. 1, and within these clades, major geographic structuring is depicted in Fig. 2a, b.

Morphological analysis

The final morphological dataset (adults only) contained 13 *P. undata* "North" (7 males, 6 females), 20 *P. inornata* "Central" (15 males, 5 females), 22 *P. inornata* "South" (15 males, 7 females), 10 *P. rubens* (4 males, 6 females), 21 *P. gaerdesi* (8 males, 13 females), and 11 *P. undata* "South" (2 males, 9 females). We ran Shapiro-Wilk normality tests on all meristic characters and found that only Gu data was normally distributed ($W = 0.9838$, $p = 0.2782$) and met the assumption of homogeneity of variance (Levene's test, $F = 1.8392$, $p = 0.113$), whereas all other characters were not normally distributed: G ($W = 0.95389$, $p = 0.0018$), Su ($W = 0.56256$, $p < 0.001$), IF ($W = 0.74376$, $p < 0.001$), SuL ($W = 0.95704$, $p = 0.0044$), Fe ($W = 0.93945$, $p < 0.001$) (see Suppl. material 6: Table S3 for detailed results).

Using ANOVA or Kruskal-Wallis rank sum tests (and subsequently applied Wilcoxon rank sum test) we found significant differences only in the number of subdigital lamellae on the fourth toe (SuL; Kruskal-Wallis chi-squared = 11.603, $p = 0.0407$) and the number of femoral pores on the leg (Fe; Kruskal-Wallis chi-squared = 24.992, $p < 0.001$) between the species of the *P. undata* complex. Since none of these differences contribute meaningfully to the diagnosis of the new taxa we present the data in the Suppl. material 7: Table S4 for reference, but refrain from overinterpreting them in this present study.

For the difficult to distinguish species pairs *P. undata* "North" and *P. undata* "South", as well as *P. inornata* "Central" and *P. inornata* "South", we assessed mensural characters in an allometric context by comparing their linear regressions (see Suppl. material 8: Fig. S1, Suppl. material 9: Fig. S2 for linear regression comparisons of mensural characters). However, in our dataset, the average SVL of adult *P. inornata* ("Central") and *P. inornata* ("South") were significantly different, with *P. inornata* ("Central") being significantly smaller (Wilcoxon rank sum test, $W = 122$, $p = 0.01401$), preventing a meaningful comparison of all other size-related body measurements by this method. While the similar-sized *P. undata* ("North") and *P. undata* ("South") (Wilcoxon rank sum test, $W = 78$, $p = 0.728$), might differ with regard to forelimb length (FoL) and lower jaw length (JL) (see Suppl. material 8: Fig. S1), this may be due to other factors (e.g. sampling bias, potential sexual size dimorphism), but limited sample sizes prevented the use of multivariate analyses for clarification.

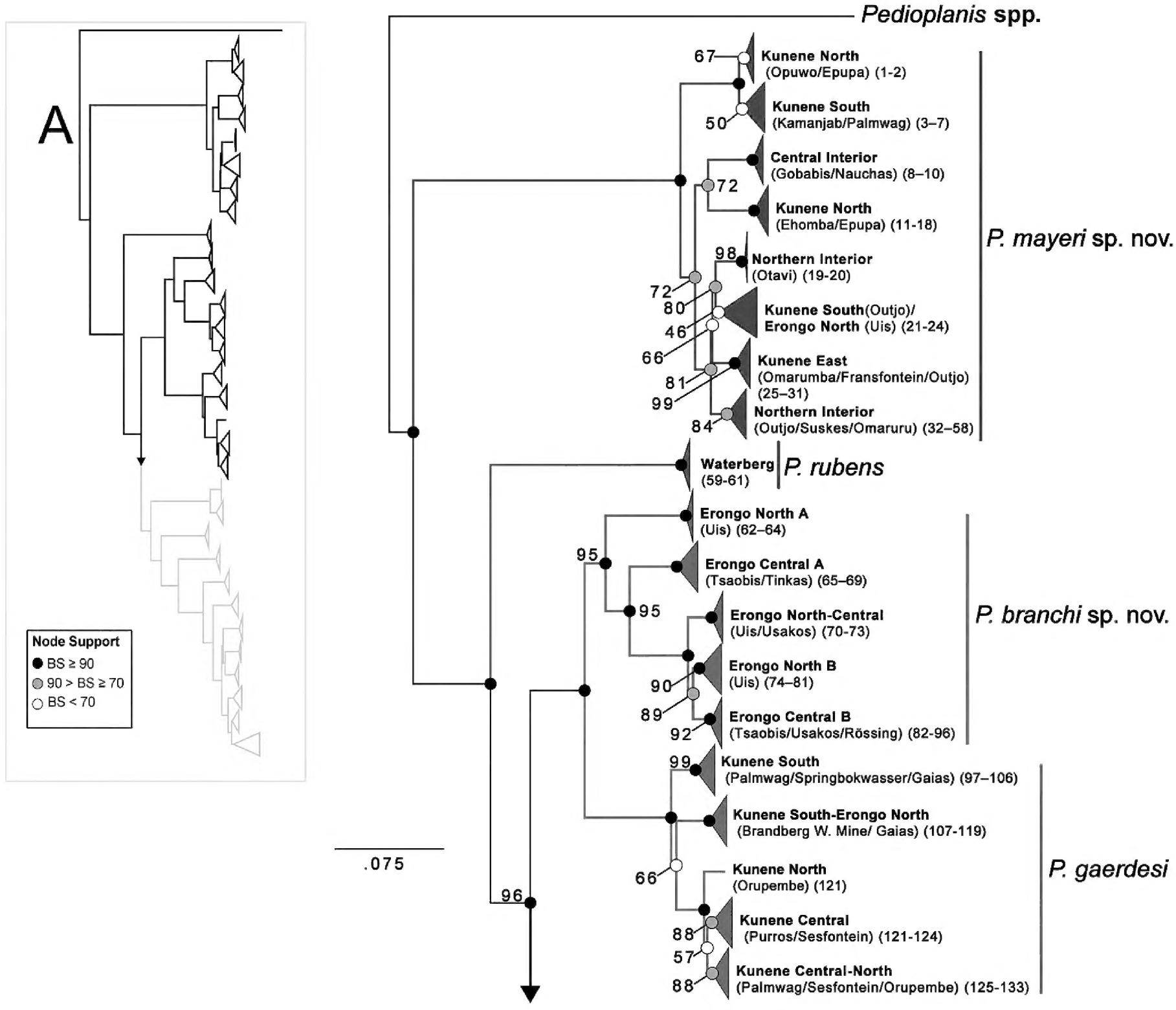

Figure 2. Maximum likelihood phylogeny of the *Pedioplanis undata* species complex inferred from the concatenation of the two mitochondrial genes ND2 and cyt *b*. Major geographically-structured clades are depicted for each species: (**a.**) *P. branchi* sp. nov. (yellow), *P. gaerdesi* (green), *P. mayeri* sp. nov. (teal), *P. rubens* (brown), (**b.**) *P. inornata* (blue) and *P. undata* (orange). Triangles indicate multiple sampled specimens. Locality names in bold refer to more inclusive area represented by the clade, parenthetical place names are main specific localities. Number ranges correspond to the sample numbers in Suppl. material 1: complete list of of tissue specimen and GenBank sampling. Node support labels are represented by bootstrap values (BS), with black nodes denoting BS ≥ 90, gray nodes denoting 90 > BS ≥ 70, and white nodes denoting BS < 70; bootstrap values of 100 are not shown.

Systematics

Our phylogenetic results support the existence of two highly divergent, unnamed entities within the *P. undata* species complex, each previously recognized as a putatively distinct, but unnamed lineage of a recognized taxon (*P. undata* and *P. inornata*). The results of the phylogenetic analyses further indicate that these lineages exhibit species-level genetic differentiation and, on this basis, we elevate the *P. undata* "North" clade and the *P. inornata* "Central" clade to full species, which we describe here using the general lineage concept of species (de Queiroz 1998).

Pedioplanis undata "South"/*P. undata* "North"

Mayer and Böhme (2000) examined the type material of *Lacerta undata* Smith, 1838 and noted that the rediscovered syntype specimens in the National Museums of Scotland collection were, in fact, representatives of the taxon long associated with the name *Pedioplanis lineoocellata pulchella* (Gray, 1845) and now, based on the findings of Edwards (2013), considered as *P. lineoocellata* (Duméril & Bibron, 1839). They proposed to conserve the current usage of names within *Pedioplanis* by calling on the ICZN in Case 3085 to set aside the original type designation and recognize the designation of a neotype for *L. undata*. Opinion 1992 of the ICZN (Anonymous 2002) accepted this solution and thus the neotype was fixed as Naturhistorisches Museum Wien (NMW) 31886 from "near Windhoek, Namibia." This links the name *P. undata* to the *P. undata* "South" clade. The assignment of the name *Pedioplanis undata* to the more restricted, southern clade is notable in that the predominant concept of the species based on previous studies of *P. undata*

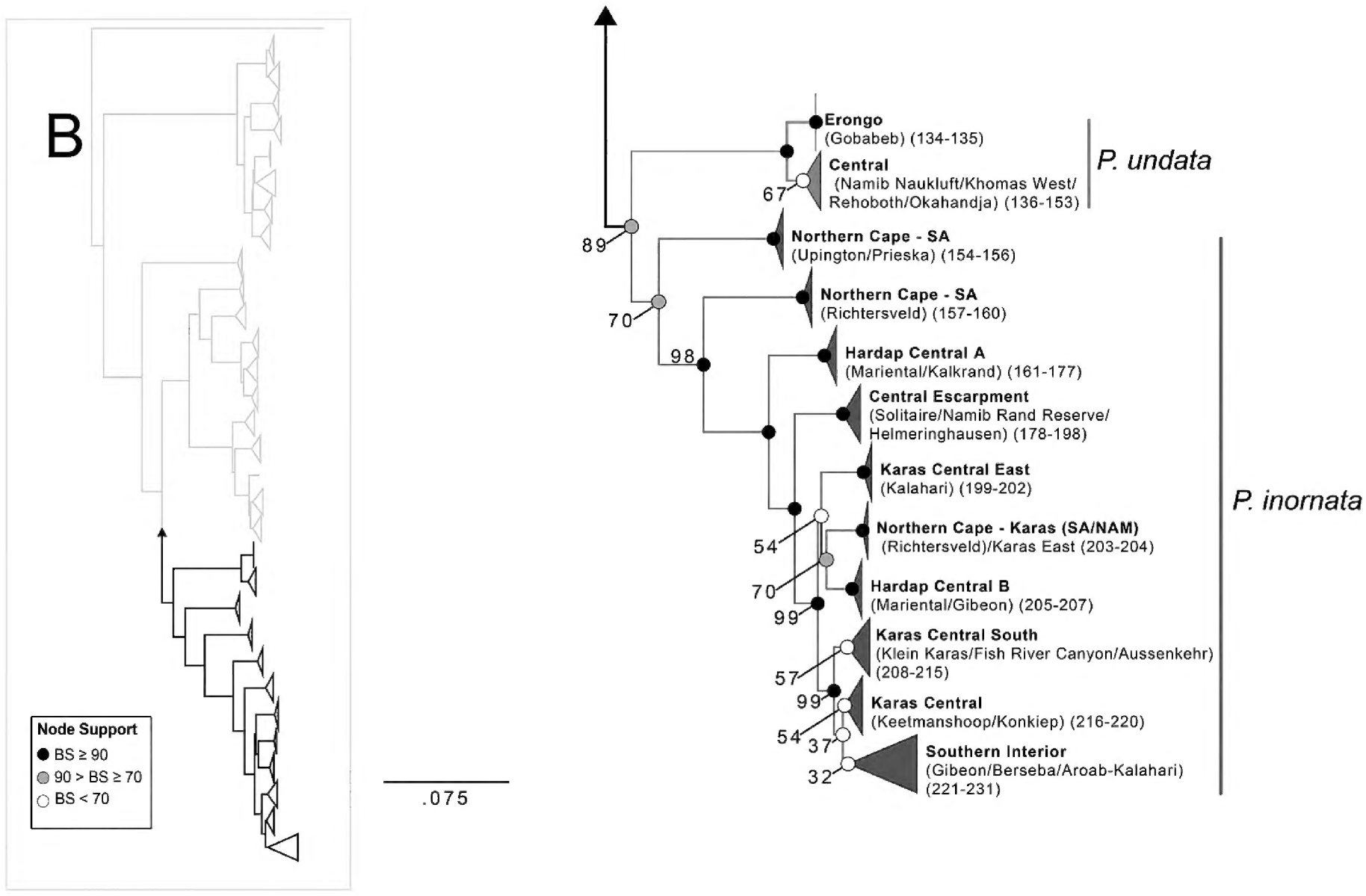

Figure 222. Continued.

is largely affiliated with populations and representative specimens from the more broadly distributed northern clade (Branch 1998; Makokha et al. 2007; Conradie et al. 2012). In these cases the presence of bold dorsal stripes was considered diagnostic for the species, however based on our results this character is now largely applicable to the unnamed northern clade, and is exhibited inconsistently and with variation among true *P. undata*. No other nomina are currently within the synonymy of *Pedioplanis undata* and none are available for application to the *P. undata* "North" clade, which we describe as:

***Pedioplanis mayeri* sp. nov.**

http://zoobank.org/1EDAC87A-1018-4A70-82BF-B9A0040D0E86

Figs 3–5

Holotype (Fig. 3). • Adult ♀; MCZ-R193179 (field number MCZ-A28704); Namibia, Erongo Region, Omaruru District, at Farm Omandumba, ca. 1 km W of house (-21.49786, 15.62630, 1238 m above sea level (a.s.l.)); collected 15 June 2014 by Jackie L. Childers, Aaron M. Bauer, William R. Branch, Matthew Heinicke and Johan Marais. Holotype and part of type series to be transferred to the National Museum of Namibia.

Paratypes. n = 8 (all specimens are adults unless otherwise noted); three ♀: CAS 214643, MCZ-R185872, ZMB 89349; five ♂: CAS 214645, MCZ-R185870, MCZ-R190213, MCZ-R193125, ZMB 89350 collected from various localities in the Kunene Region of northern Namibia • CAS 214643; 59 km W of Kamanjab (-19.64871, 14.33984, 1163 m a.s.l.); collected 1 June 2000 by Aaron M. Bauer • CAS 214645; same collection data as for proceeding • MCZ-R185870; 35 km S of Epupa Falls on Okangwati Rd. (-17.26083, 13.21194, 1035 m a.s.l.); collected 14 August 2007 by Aaron M. Bauer, Johan Marais, Ross A. Sadlier, and Stuart V. Nielsen • MCZ-R185872; N Okangwati on Epupa Falls Rd. (-17.40361, 13.15861, 1140 m a.s.l.); collected 14 August 2007 by Aaron M. Bauer, Johan Marais, Ross A. Sadlier, and Stuart V. Nielsen • MCZ-R190213; ca. 4 km from Swartbooisdrif towards Epembe (-17.38136, 13.82955, 836 m a.s.l.); collected 27 November 2011 by Aaron M. Bauer • MCZ-R193125; collected at the type locality on 13 June 2014 • ZMB 89349; subadult ♀; along the C35 road, ca. 2 km N of Fransfontein (-20.19976, 15.01453, 1097 m a.s.l.); collected 15 August 2014 by Sebastian Kirchhof • ZMB 89350; along the C43 road, 29 km N of Palmwag (-19.62736, 13.87391, 1124 m a.s.l.); collected 15 August 2014 by Sebastian Kirchhof. Elevation data for the holotype and paratypes was obtained using the GPS or, if not available, from Google Earth (earth.google.com) using georeferenced GPS coordinates from the collecting localities.

Diagnosis. Distinguished from *P. lineoocellata*, *P. laticeps* and *P. burchelli* by having 10 longitudinal ventral scale rows (vs. 12 or more). It is distinct from *P. gaerdesi*, *P. benguelensis*, *P. husabensis*, *P. namaquensis* and *P. breviceps* in possessing a semi-transparent lower eyelid with a brille formed by 2–4 enlarged scales (brille formed by a single scale in *P. benguelensis* and *P. gaerdesi*, lower eyelid with eight opaque scales in *P. husabensis* and

opaque and scaly in *P. breviceps* and *P. namaquensis*). Dorsal patterning is characterized by the presence of five, usually bold dark brown to black, straight-edged dorsal stripes, distinguishing it from *P. rubens* (dorsum and tail uniform red-brown to brick red, lacking conspicuous markings with only a hint of a slightly brighter dorso-lateral line on each side), *P. inornata*, *P. gaerdesi* and *P. branchi* sp. nov. (dorsum may be light to dark gray becoming gradually more reddish towards the tail, possessing dark and/or light beige-yellowish speckling but lacking distinct longitudinal elements), *P. haackei* (only three dark dorsal stripes), and *P. undata* (dorsal striping bold or not, may be reduced with pale longitudinal elements or even a single middorsal stripe restricted to the nape). It is further distinguished from *P. haackei* by typically having a smaller number of granules anterior to the first supraocular (9–16 vs. 12–32), from *P. huntleyi* in having a larger number of granules anterior to the first supraocular (9–16 vs. 7–13), and from *P. undata* in possessing a greater maximum number of granular scales anterior to the supraoculars (9–16 in *P. mayeri* sp. nov. versus 8–13 in *P. undata*), and a greater maximum number of femoral pores on a single leg (12–16 in *P. mayeri* sp. nov. versus 11–14 in *P. undata*) (see Suppl. material 7: Table S4 and Suppl. material 3). *Pedioplanis mayeri* is similar in most characteristics to *P. huntleyi*, which is restricted to Angola, but the latter species is typified by the restriction of the five dark dorsal stripes to the anterior half of the trunk, a condition found in only some *P. mayeri*. No single morphological character unambiguously distinguishes the allopatric species *P. mayeri*, *P. undata* and *P. huntleyi*. We therefore provide several diagnostic characters based on the mitochondrial gene ND2 in order to supplement the morphological data. *Pedioplanis mayeri* may be distinguished from all other *Pedioplanis* species in being characterized by having the amino acid histidine instead of a tyrosine at base pair 61 due to a codon change at that position. It also has the amino acid phenylalanine at base pair 223, instead of a threonine (*P. benguelensis*, *P. breviceps*, *P. haackei*, *P. huntleyi*, *P. husabensis*, *P. laticeps*, *P. lineoocellata*, *P. namaquensis*), an alanine (*P. burchelli*), or a serine (*P. branchi* sp. nov., *P. gaerdesi*, *P. inornata*, *P. rubens*, *P. undata*) due to a codon change at that position. Finally, it has the amino acid threonine due to a codon change at base pair 568, instead of a leucine (*P. rubens*), a valine (*P. haackei*, *P. laticeps*, *P. undata*), or an isoleucine (*P. benguelensis*, *P. branchi* sp. nov., *P. breviceps*, *P. burchelli*, *P. gaerdesi*, *P. husabensis*, *P. namaquensis*); *P. inornata* and *P. lineoocellata* are polymorphic with individuals possessing either valine or isoleucine, and it is unknown what the molecular character state is for *P. huntleyi* at this position.

Description of holotype. Body relatively slender; SVL 45.5 mm; interlimb distance 20.4 mm; femur 10.0 mm; tibia 9.8 mm; humerus 5.5 mm; forearm 5.8 mm; body length 28.9 mm from groin to collar; collar-snout length 16.1 mm; fourth finger length 5.7 mm; fourth toe length 11.1 mm; head narrow and elongated (head width 52% of head length) with narrow pointed snout (width at rear of frontonasal 2.2 mm, width at front of eye 3.8 mm); head length 11.0 mm; head width 5.7 mm; lower jaw length 8.5 mm; eye–ear distance 4.1 mm; eye–nostril distance 3.8 mm; 1.6 mm between the nostrils; original unregenerated tail 116.7 mm. Rostral semicircular, contacting nasals and supranasals; nostril surrounded by nasal, supranasal, and postnasal; nasals unraised relative to rostral and frontonasal; postnasal contacts nasal, supranasal, frontonasal, anterior loreal, and enters the nostril; nostrils circular; two loreals, anterior half the length of the posterior; two preoculars; prefrontals in median contact; frontal large, with a narrow posterior projection that contacts the frontoparietals; frontoparietals in medial contact; interparietal in contact anteriorly with both frontoparietals, laterally with the parietals, and posteriorly with the occipital; occipital partially fused with parietals at posterior margin; two supraoculars, both in contact with the frontal, preceded anteriorly by a group of 15R/16L granules, two granules in contact with prefrontal and two in contact with frontal (L); one granule in contact with prefrontal and two in contact with frontal (R); two rows of granules dividing anterior supraocular from supraciliaries; three small scales between last supraciliary and parietal; six supraciliaries on each side, anterior-most longest; lower eyelid with transparent brille formed of two larger, black-edged scales, with a row of five smaller scales below; five supralabials anterior to subocular and three supralabials posterior to subocular, on both sides; subocular bordering lip, its lower edge narrower than its upper; 6R/6L infralabials; first infralabial in contact with the second infralabial, the first chin shield, and the mental; four enlarged pairs of chin shields, the first three in median contact and enlarging progressively to the posterior; two enlarged temporals; tympanum sunken; no scales projecting significantly past margin of ear opening; enlarged narrow scale at anterodorsal margin of tympanum. 28 gular scales in a straight line between symphysis of chin shields and median collar plate; collar free, comprising 11 enlarged plates (median trapezoidal) and extending onto side of neck as a crease that terminates midway up the lateral surface; dorsal scales small, juxtaposed, granular, without keels, lateral scales becoming increasingly larger ventrally; 53 rows of granular scales around the midbody; ventral plates in 10 longitudinal and 30 transverse rows (from collar to groin); ventral scales squarish, subimbricate; single transverse row of ventrals across chest just posterior to collar longer than broad; 11 enlarged precloacal scales, irregularly sized; scales on upper surface of forearm large, smooth, and overlapping, without keels; scales on lower surface of forearm with a series of enlarged plates, at least twice width of scales on upper forearm; scales on upper surface of tibia rhombic, subimbricate and distinctly keeled, below with a series of enlarged plates; scales on upper surface of femur keeled with enlarged scales along the anterior margin; 15 femoral pores on each side; 27 subdigital lamellae under fourth toe; scales on tail uniform,

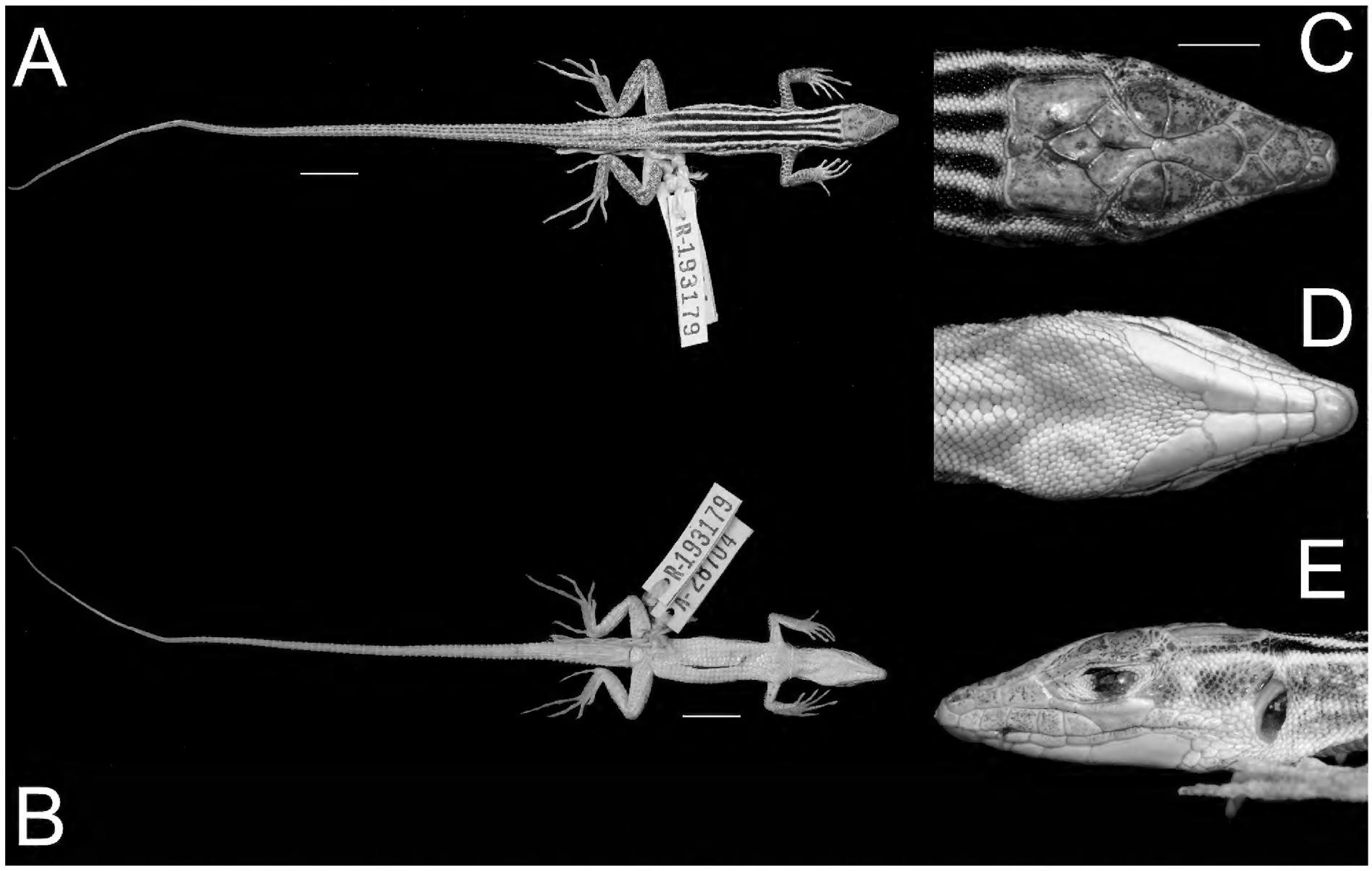

Figure 3. *Pedioplanis mayeri* sp. nov. adult female holotype (MCZ-R193179) from Farm Omandumba in the Erongo Region of Namibia. (**a.**) Dorsal and (**b.**) ventral views of the whole body; scale bars indicate 10 mm; (**c.**) dorsal, (**d.**) ventral) and (**e.**) lateral views of the head; scale bar indicates 2.0 mm.

obliquely rectangular in shape, and strongly keeled; 24 presacral vertebrae.

Color in alcohol. Dorsum of crown gray-tan with small speckles of varying size on head shields; dorsum of snout tinged with reddish-brown. Lateral surface of head cream-colored with minute gray speckles on loreal scales, supralabials and infralabials. Granules bordering lower eyelid window white. Color and pattern of temporal region confluent and consistent with those on trunk. Trunk dorsum with three bold black stripes each bordered on either side by whitish-cream stripes that extend to the sacrum, becoming indistinct on the tail; middorsal black stripe divided anteriorly by a whitish–cream stripe that extends from the occiput to the level of the forelimb insertion, narrowing from a width of five granular dorsal scales to two from anterior to posterior. Below the lateralmost of these pale stripes, which originates on the temporal, lies a thick darkly pigmented line to which is fused the coalescence of a series of 9R/8L irregularly sized ocelli with pale gray-blue centers comprising 6–14 granules, each surrounded by a brown to black ring. This in turn is bordered ventrally by a diffuse white line which begins at the corner of the mouth, passes through the ear and continues to the groin. Below this line the flanks transition to the immaculate pearly white of the venter. Dorsal surfaces of forelimbs mottled brown with margins of enlarged scales pale; dorsal surfaces of hind limbs medium brown, enlarged scales on preaxial surface similar to those of forelimb, postaxial surfaces bearing scattered cream-colored spots, each 1–3 granular scales in extent; palms and soles gray with scattered diffuse pinkish to orange markings. Tail light brown, densely speckled with darker markings which continue the bold lateral black stripes of the body dorsum as a pair of narrow dark brown stripes running along the medial-most keels of the tail for at least three quarters of its length.

Variation within the type series. Measurements for the type series are summarized in Table 1 and mensural (n = 13) and meristic (n = 17) character data based on measurements of additional museum vouchers can be found in Suppl. material 2, 3, respectively. Paratypes have similar scalation to the holotype except as follows: in MCZ-R185872 the prefrontals do not contact and are instead divided by a granule; in MCZ-R193125 the interparietal and occipital are separated by a granule; in all paratype specimens the occipital is not fused with the parietals; the number of granules in the group preceding the anterior supraocular varies from nine to 15; in CAS 214645 and ZMB 89349 there is one row of granules dividing the anterior supraocular from the supraciliaries (usually two); in CAS 214645 and MCZ-R185870 there are 7R and 7L infralabials, respectively (usually six); gular scales in a straight line between the symphysis of chin shields and the median collar plate varies from 27 to 32; midbody scale rows vary from 57 to 64; subdigital lamellae under the fourth toe range from 25 to 28; unilateral

Table 1. Morphological data for *Pedioplanis mayeri* sp. nov. type series. CAS = California Academy of Sciences, MCZ = Museum of Comparative Zoology, ZMB = Museum für Naturkunde. Abbreviations for character values are as follows: C = In contact; S = Separated by granule; SF = Separated by frontal and frontonasal; INC = Tail incomplete. See Materials and Methods for character abbreviations and descriptions; Midbody scale rows (MB) were not recorded for all individuals.

Type Status	Holotype	Paratype	Paratype	Paratype	Paratype	Paratype	Paratype	Paratype	Paratype
Museum No.	MCZ-R 193179	CAS 214643	MCZ-R 185872	ZMB 89349	CAS 214645	MCZ-R 185870	MCZ-R 190213	MCZ-R 193125	ZMB 89350
Sex	Female	Female	Female	Female	Male	Male	Male	Male	Male
SVL (mm)	45.5	40.7	47.0	43.3	44.0	51.4	49.2	43.5	52.7
TaL (mm)	116.7	NA (INC)	108.5	105.4	107.3	124.9	131.8	96.4	121.5
PF	C	C	S	C	C	C	C	C	C
G	16	9	11	15	14	10	11	10	13
RG	2	2	2	1	1	2	2	2	2
Su	6	6	6	6	6	6	6	6	6
IO	C	C	C	C	C	C	C	S	C
IF	6	6	6	6	6L/7R	7L/6R	6	6	6
Gu	28	28	29	28	31	27	29	31	29
SuL	27	25	25	26	27	28	27	26	26
Fe	15	13	14	13	14	14	14	14	13
PV	24	25	24	25	24	24	24	25	24
MB	–	–	61	–	57	64	64	58	–

femoral pores number 13 to 14 (right side only); and presacral vertebrae number either 24 or 25.

Coloration in life (Fig. 4). Dorsal coloration and pattern varied considerably across examined specimens. Dorsum of head gray-tan, sometimes possessing dark speckles of varying size; dorsum usually bearing three bold black, medium-brown or gray stripes bordered on each side by white stripes; dorsal stripes often terminate at the tail base or begin to fade into a gray and reddish hue midway towards the tail base; dorsal stripes may be absent entirely, with individuals possessing a uniformly gray dorsum, sometimes with dark speckling. All individuals examined possess yellow-centered ocelli or yellow spots along the flanks, usually bordered ventrally by a white stripe and dorsally by a black stripe (or with the dark rims of the ocelli confluent with such a stripe); lateral spots or ocelli vary in size from ca. 0.5 to 1.0 mm in diameter, in some cases smaller spots may merge with the white ventral stripe; anterior surface of the thighs and outermost ventral plates sometimes tinged or speckled with orange; limbs and feet more or less uniformly grayish (front), reddish-brown to brown, or speckled with light or black dots or blotches that may form bars; tail usually bright brick or orange-red, in some cases dark speckling may be present on the dorsal surface of the tail.

Coloration in alcohol. Pattern as described above though dark stripes may fade to dark gray, yellow lateral spots may appear cream white or gray-blue, and red coloration usually present on the dorsum of the midbody and tail may become a faded orange-pink or may fade to a faint, golden-brown hue.

Distribution. *Pedioplanis mayeri* sp. nov. is endemic to northern Namibia and occurs from south of the Kunene River and east of the Namib Desert along the eastern side of the escarpment, thence throughout the eastern Kunene Region, entering the northeastern parts of the Erongo Region and east through the Otjozondjupa Region, reaching at least as far east as Oshikango (TM17028) in the north, Gobabis (Omaheke Region) in the south-east, and Nauchas in the south. It does not enter the Kalahari dune fields, and is possibly absent from the Khomas Hochland, where it is replaced by *P. undata* (see Fig. 6 for map of locality records).

Etymology. The specific epithet is a patronym formed in the genitive singular honoring our friend and colleague, the Austrian lacertid specialist Werner Mayer (1943–2015), who first recognized the distinctiveness of his namesake species and whose contributions to the study of *Pedioplanis* have been seminal.

Natural history. *Pedioplanis mayeri* is widespread in northern Namibia and inhabits Tropical & Subtropical Grasslands, Savannas & Shrublands and Deserts & Xeric Shrublands biomes (following the classification of the WWF; Olson et al. 2001), but it is absent from true desert. Within the occupied biomes, *P. mayeri* inhabits Namibian savanna woodlands, Kalahari xeric savanna, Kalahari Acacia-Baikiaea woodlands and Angolan Mopane woodlands (terminology follows Olson et al. 2001). Here, the species is active on sandy clay soils and more compact, hard soils, rocky flats and slopes, in dense grassy patches as well as in more open areas interspersed with shrubs (see Fig. 5 for images of characteristic habitats). In rocky areas and stony slopes individuals were found sleeping under stones. The majority of the species' range comprises Namibia's arid regions with a median annual precipitation of 279 mm (61–559 mm) and a median annual temperature average of 21.1 °C (18–23.5 °C) (all climate data taken from Fick and Hijmans 2017). *Pedioplanis mayeri* mainly occurs along the northern parts of the Great Escarpment at a median elevation of 1160 m a.s.l., but reaches altitudes as high as ca. 1600 m a.s.l. in Otjozondjupa, and probably as low as ca. 200 m a.s.l. in the north along the Kunene River. The largest recorded individual was a female with SVL = 57 mm (see also Kirchhof et al. 2014; the individuals referred to therein as *P. undata* are now *P. mayeri*). Breeding season appears to be in spring, similar to other southern African *Pedioplanis* spp. Gravid

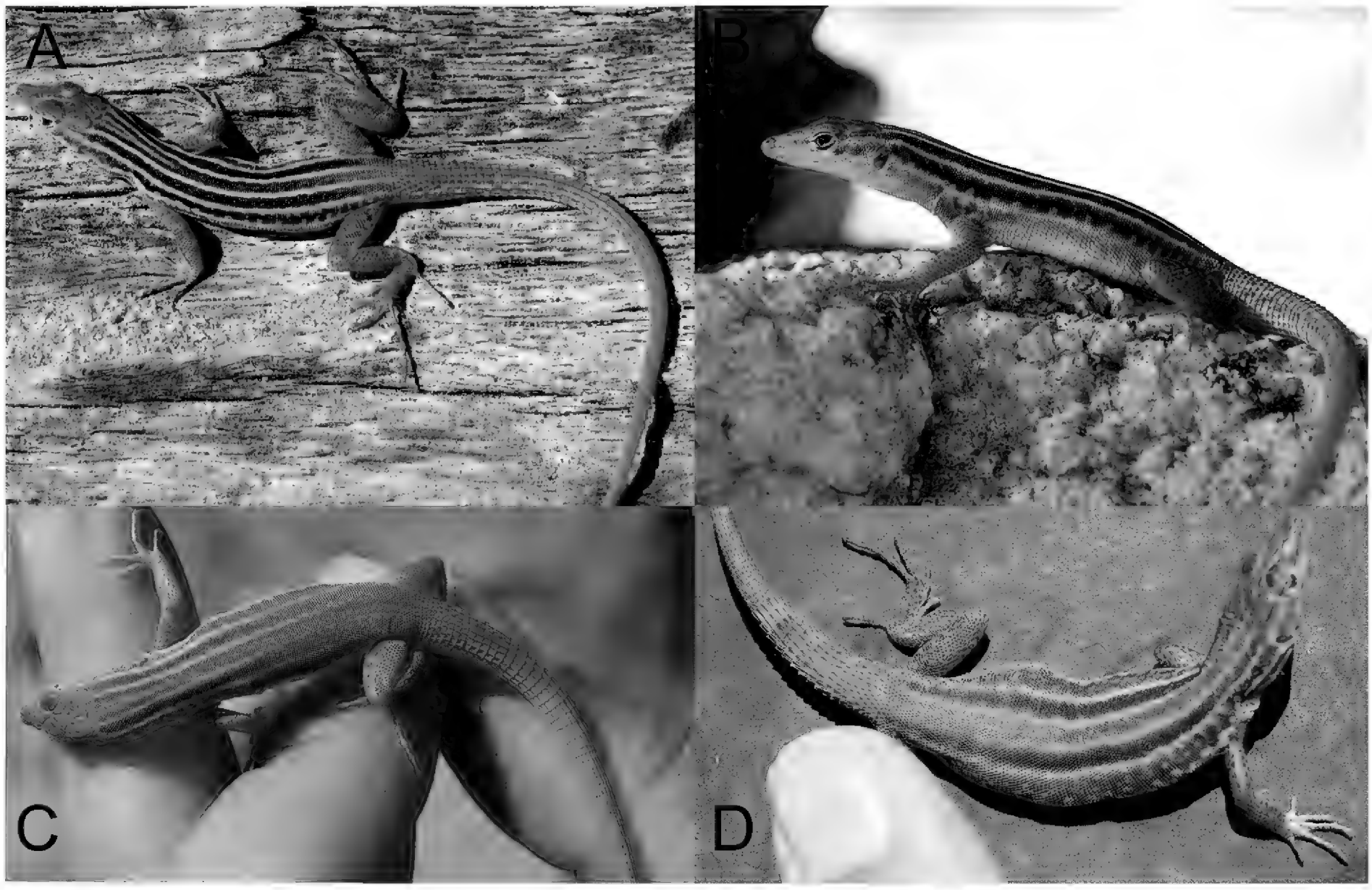

Figure 4. Life photographs of representative individuals of *Pedioplanis mayeri* sp. nov. highlighting color pattern variation within the species. (**a.**) Dorsal and (**b.**) lateral whole body images of an adult possessing bold dorsal stripes collected at the type locality (Farm Omandumba, Erongo Region, Namibia), note the row of yellow spots along the flanks; (**c.**) Dorsal image of an adult from the Kamanjab area depicting fainter, medium-brown dorsal stripes; (**d.**) An adult female collected from Gobabis (ZMB 80391; see also Fig. 5a) with dorsal striping of varying boldness and a more grayish-brown hindbody compared to the more reddish hindbody observed in other individuals.

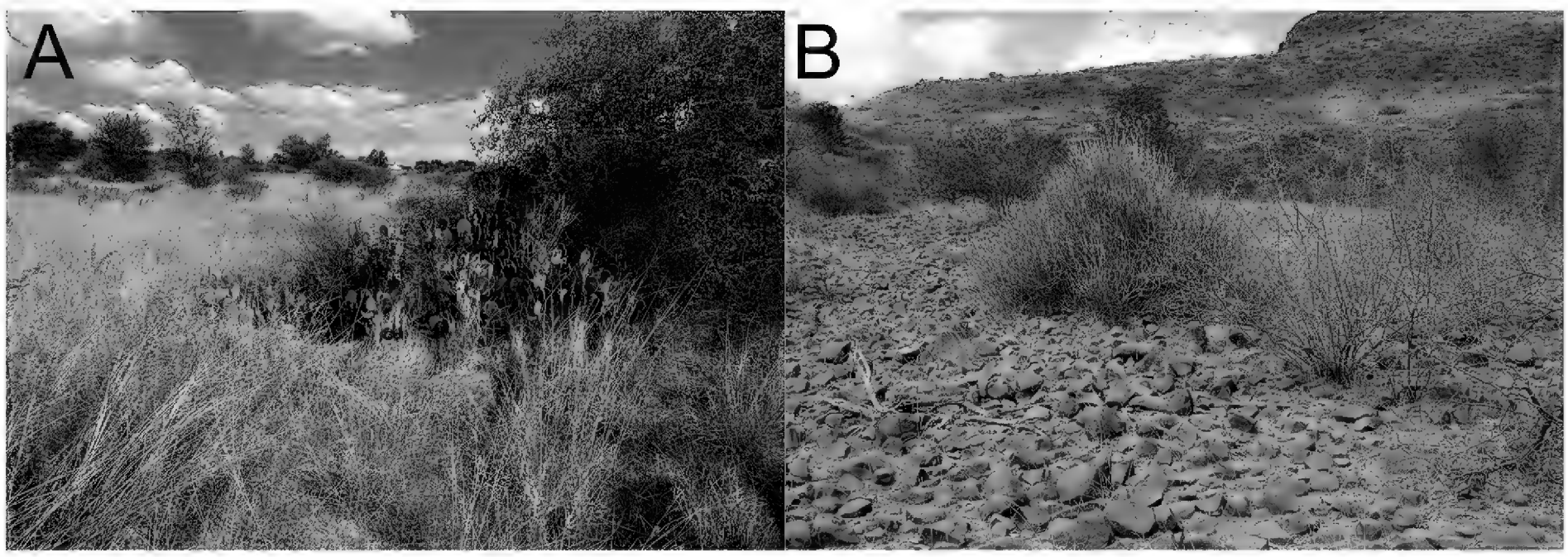

Figure 5. Habitat of *Pedioplanis mayeri* sp. nov. (**a.**) Collection site near Gobabis for ZMB 80389–80392 in open savannah woodland, with tall, dense grasses and introduced *Opuntia*. (**b.**) Collection site for ZMB 89350 (29 km N of Palmwag, Kunene Region, Namibia) in stony Pro-Namib habitat with sparse vegetation dominated by *Euphorbia damarana* (center).

females with up to four eggs were found in December and February, and small juveniles (SVL = 27 mm) appeared in mid-February (Kirchhof et al. 2014). Sympatric ground-living diurnal lizards include *Trachylepis damarana*, *Meroles squamulosus*, *Heliobolus lugubris*, *Gerrhosaurus flavigularis*, and *Agama anchietae*, among others.

Conservation. The species occurs across a wide area of Namibia in which potential threats from agriculture and mining are scattered and localized. Local populations occur in protected areas within Etosha National Park and Waterberg Plateau Park as well as in many local conservancies. Applying IUCN criteria, we consider *P. mayeri* to be Least Concern.

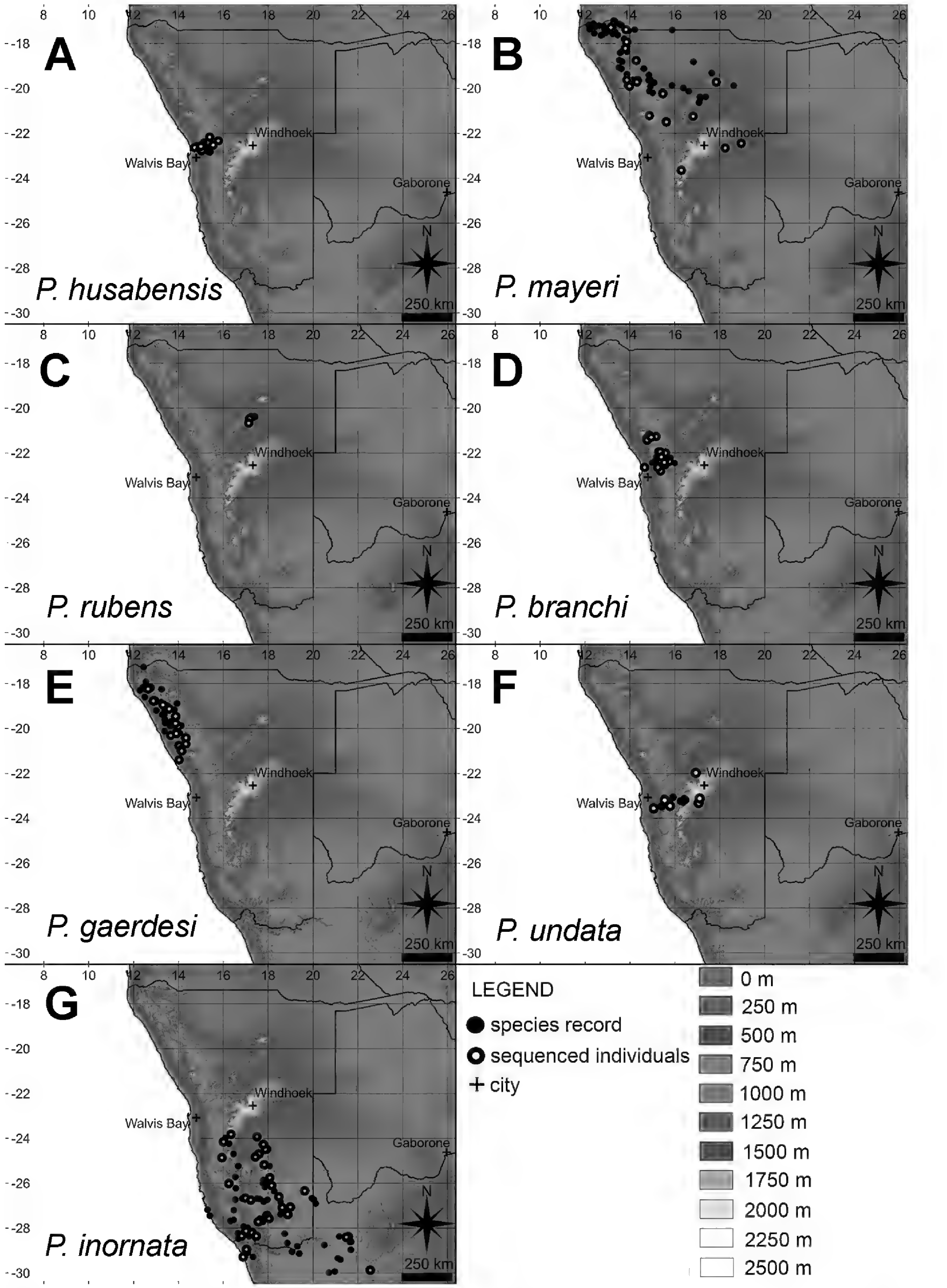

Figure 6. Topographic maps showing locality records for all the species of the *Pedioplanis undata* species complex and *P. husabensis*: (**a.**) *P. husabensis* (**b.**) *P. mayeri* sp. nov. (**c.**) *P. rubens* (**d.**) *P. branchi* sp. nov. (**e.**) *P. gaerdesi* (**f.**) *P. undata* (**g.**) *P. inornata*. Black dots represent museum vouchers from various museum collections, those with a white center were sequenced and included in the phylogenetic analyses. Museum voucher information was collected from the California Academy of Sciences San Francisco/USA, Carnegie Museum of Natural History Pittsburgh/USA, Ditsong National Museum Pretoria/South Africa, Iziko South African Museum Cape Town/South Africa, Museum für Naturkunde Berlin/Germany, Museum of Comparative Zoology Harvard University/USA, Museum of Vertebrate Zoology Berkeley/USA, Natural History Museum of Los Angeles County/USA, Bayworld Museum Port Elizabeth/South Africa, National Museum of Namibia Windhoek/Namibia, Zoological Research Museum Alexander Koenig Bonn/Germany, in parts via the Global Biodiversity Information Facility (GBIF; https://www.gbif.org/).

Pedioplanis inornata "South"/*P. inornata* "Central"

The type series of *Eremias inornata* Roux, 1907 comprises eight specimens collected from "Oranje-Fluß, Kl.-Namaqualand" [the Orange River, Little Namaqualand, Northern Cape, Province, South Africa]. Syntype ZMA11049 (Zoological Museum Amsterdam) was subsequently designated as the lectotype (Daan and Hillenius 1966). The ZMA collections have subsequently been incorporated into those of the Naturalis Biodiversity Center in Leiden (RMNH). The geographic origin of the specimens and the relatively detailed description and accompanying plate, clearly tie the name-bearing lectotype of *Pedioplanis inornata* to the *P. inornata* "South" clade. No other nomina are currently within the synonymy of *Pedioplanis inornata* and none are available for application to the *P. inornata* "Central" clade, which is here described as:

Pedioplanis branchi sp. nov.

http://zoobank.org/7FDBC1FF-BEB4-464A-88C5-6CDD19ED50F2

Figs 7–9

Holotype (Fig. 7). Adult ♂; CAS 214788 (field number AMB 6551); Namibia, S of Karibib at Junction of Road D1914 and Road D1952, Karibib District, Erongo Region (-22.27038, 15.57471, 1080 m a.s.l.); collected 8 June 2000 by Aaron M. Bauer. Holotype and part of type series to be transferred to the National Museum of Namibia.

Paratypes. n = 7 (adults); (two ♀: ZMB 89310, ZMB 89311; five ♂: CAS 214790, CAS 214792, CAS 214794, ZMB 89305, ZMB 89316) collected from various localities located in the Erongo Region of northwestern Namibia • CAS 214790; S of Karibib at the junction of Rd. D19414 and Rd. D1952 (-22.27281, 15.57815, 1075 m a.s.l.); collected 8 June 2000 by Aaron M. Bauer • CAS 214792; same collection data as for proceeding • CAS 214794; same collection data as for proceeding • ZMB 89305; 22 km SW of Uis along C35 (-21.42419, 14.76271, 831 m a.s.l.); 10 August 2014 • ZMB 89316; 22 km SW of Uis along C35 (-21.34513, 14.75676, 884 m a.s.l.); 23 January 2013 • ZMB 89310; Farm Friedhelm Sack (-22.52699, 15.54487, 709 m a.s.l.); 14 October 2014; • ZMB 89311; same collection data as for proceeding; all ZMB specimens collected by Sebastian Kirchhof. Elevation data for the holotype and paratypes was obtained using the GPS, or, if not available, from Google Earth (earth.google.com) using georeferenced GPS coordinates from the collecting localities.

Diagnosis. Distinguished from *P. lineoocellata*, *P. laticeps* and *P. burchelli* by having 10 longitudinal ventral scale rows (vs. 12 or more). It is distinct from *P. benguelensis*, *P. gaerdesi*, *P. breviceps*, *P. namaquensis* and *P. husabensis* in usually possessing a semi-transparent lower eyelid with a brille formed by 2–4 scales (brille formed by a single scale in *P. benguelensis* and *P. gaerdesi*, lower eyelid with eight opaque scales in *P. husabensis* and opaque and scaly in *P. breviceps* and *P. namaquensis*); in some rare cases *P. branchi* sp. nov. may possess a single transparent scale in lower eyelid, those individuals can be distinguished from *P. benguelensis* and *P. gaerdesi* by color and dorsal patterning (see below). Dorsal patterning is characterized as being uniformly gray from the mid-back towards the head with a reddish hindbody (posterior half of body) and with a series of pale to bright yellow spots or ocelli on lower flanks, distinguishing it from *P. rubens* (dorsum and tail uniform red-brown to brick red, lacking conspicuous markings with only a hint of a slightly brighter dorso-lateral line on each side), *P. mayeri* sp. nov., *P. haackei*, *P. huntleyi*, *P. undata* (dorsum contains bold stripes or other longitudinal elements), *P. gaerdesi* (never with lateral ocelli, and speckled with very small black or light dots) and *P. inornata* (spots on flanks are typically pale green, not yellow). It can further be distinguished from all other *Pedioplanis* (except *P. inornata*) in typically having a pair of distinct dark markings on the face, one through the eye and extending onto the supralabials directly below and one more posterior, near the corner of the mouth. The new species is significantly smaller than *P. inornata* (*P. branchi* mean adult SVL = 44.4 mm, max. 49.1 mm, versus *P. inornata* mean adult SVL 47.3 mm, max. 54.0 mm for specimens sampled here; to 56.0 mm elsewhere [Bauer and Shea 2006]). The maturity of specimens was confirmed by their mostly or completely fused long bone epiphyses. We also provide several diagnostic characters based on the mitochondrial gene ND2. *Pedioplanis branchi* sp. nov. can be distinguished from all other members of the *P. undata* species complex except *P. laticeps* and *P. undata* in being characterized by having the amino acid histidine instead of tyrosine at base pair 359 due to a codon change at that position. It can also be distinguished from all other *Pedioplanis* species except *P. laticeps* in possessing a thymine at base pair 300, rather than an adenine (*P. benguelensis*, *P. burchelli*, *P. gaerdesi*, *P. haackei*, *P. huntleyi*, *P. husabensis*, *P. inornata*, *P. mayeri* sp. nov., *P. namaquensis*, *P. rubens*, *P. undata*) or a cytosine (*P. breviceps* and *P. lineoocellata*).

Description of holotype. Body relatively slender (SVL 47.5 mm); interlimb distance 16.8 mm; femur 9.5 mm; tibia 8.7 mm; humerus 5.4 mm; forearm 5.7 mm; body length 26.9 mm from groin to collar; collar-snout length 19.3 mm; fourth finger length 4.7 mm; fourth toe length 10.4 mm; head narrow and elongated (head width 55% of head length) with slight constriction at base of rostrum and narrow, pointed snout (width at rear of frontonasal 2.2 mm, width at front of eye 4.4 mm); head length 11.8 mm; head width 6.6 mm; lower jaw length 10.2 mm; eye–ear distance 4.4 mm; eye–nostril distance 4.0 mm; 1.1 mm between the nostrils; complete original tail 92.3 mm, with epidermis missing from posterior portions. Rostral semicircular; contacting nasals; nasals in contact medially, unraised relative to rostral and frontonasal; postnasal contacts nasal, frontonasal, anterior loreal, and enters the nostril; nostrils circular in shape; two loreals, anterior loreal half the length of the posterior loreal; two

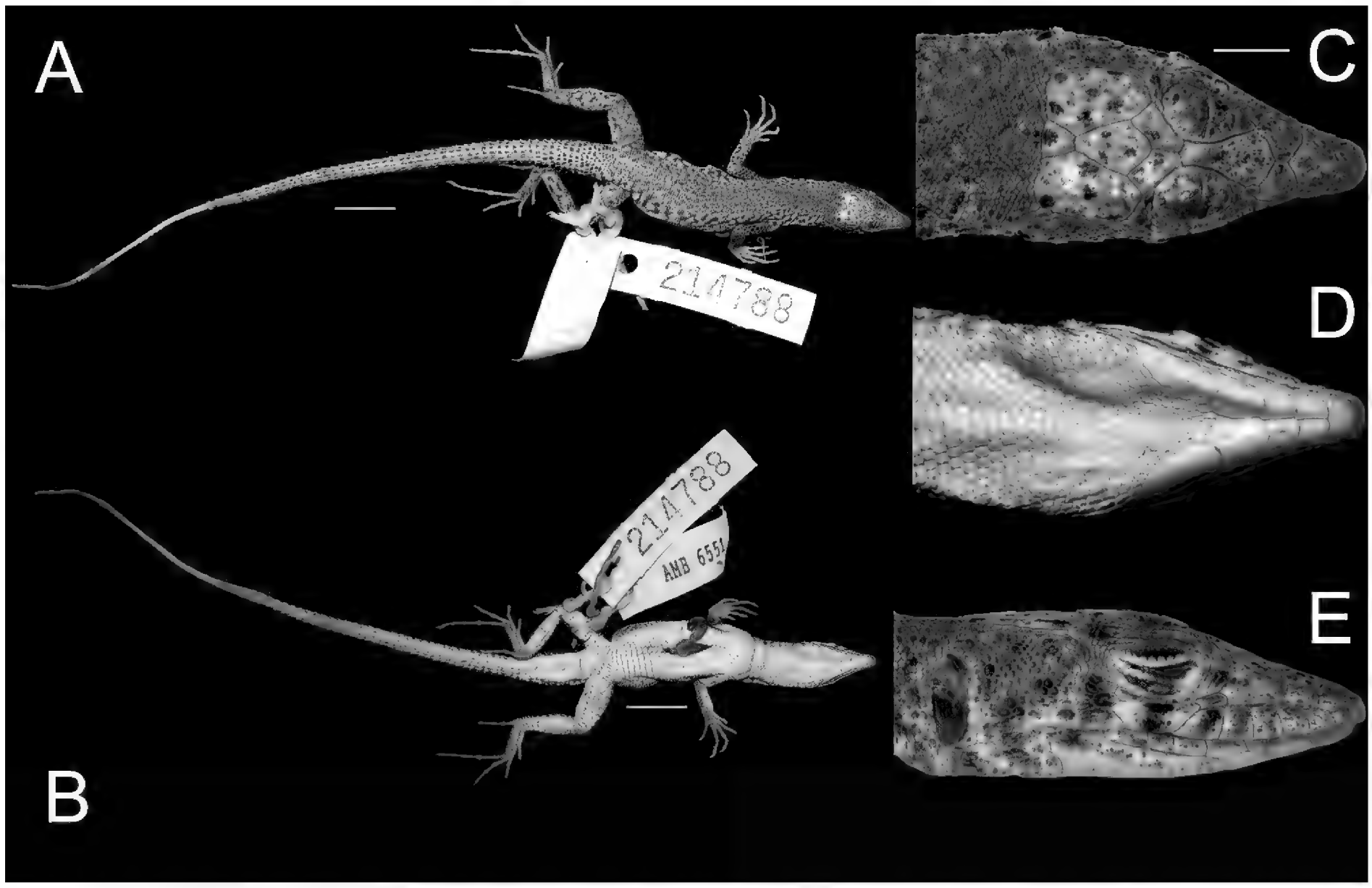

Figure 7. *Pedioplanis branchi* sp. nov., adult male holotype (CAS 214788) from south of Karibib in the Erongo Region of Namibia. (**a.**) Dorsal and (**b.**) ventral views of the whole body; scale bars indicate 10 mm; (**c.**) dorsal, (**d.**) ventral) and (**e.**) lateral views of the head; scale bar indicates 2.0 mm.

preoculars; prefrontals in median contact; frontal large, with a narrow posterior projection, bordered anteriorly by the prefrontals and posteriorly by the frontoparietals; frontoparietals in broad medial contact; interparietal in contact anteriorly with both frontoparietals, laterally with the parietals, and posteriorly with the occipital; occipital trapezoidal in shape; two supraoculars, both in medial contact with the frontal and frontoparietals, preceded anteriorly by 8R/8L granules (on left side two granules in contact with prefrontal and one in contact with frontal; on right side two granules in contact with prefrontal and three in contact with frontal); single row of granules dividing anterior supraocular from supraciliaries, and double row of granules dividing posterior supraocular from supraciliaries; two small scales between last supraciliary and parietal; six supraciliaries on each side, the anteriormost longest; lower eyelid with transparent brille formed of two larger, black-edged scales, with a row of five smaller scales beneath; five supralabials anterior to subocular and three supralabials posterior to subocular, on both sides; subocular bordering the lip, its lower edge shorter than its upper; 6R/6L infralabials; first infralabial in contact with the second infralabial, the first chin shield, and the mental; four enlarged pairs of chin shields, with the first three in medial contact and the posterior-most largest; no enlarged temporals; tympanum sunk; no scales projecting significantly past margin of ear opening; enlarged narrow scale at anterodorsal margin of ear opening. 30 gular scales in a straight line between symphysis of chin shields and median collar plate; collar free, comprising nine enlarged plates (median kite-shaped, projecting posteriorly) and extending onto side of neck as a crease that terminates midway up the lateral side; dorsal scales small, juxtaposed, granular, without keels, lateral scales larger towards ventrals; 49 rows of granular scales around the midbody; ventral plates in 10 longitudinal and 31 transverse rows (from collar to groin); plates of the outermost rows squarish, ventral rows usually twice as wide as long; single transverse row of ventrals across chest just behind collar longer than broad; nine enlarged precloacal scales, irregular in shape, median ones larger; centralmost enlarged precloacal in contact with six other enlarged precloacals; scales on upper surface of forearm large, smooth, and overlapping, without keels; scales on lower surface of forearm with a series of enlarged plates, at least twice the width of scales on upper forearm; scales on upper surface of tibia rhombic, subimbricate and distinctly keeled, below with a series of enlarged plates; scales on upper surface of femur granular and smooth with enlarged scales along the anterior margin; 12R/12L femoral pores; subdigital lamellae under fourth toe 26R/28L; scales on tail obliquely rectangular in shape, and strongly keeled.

Color in alcohol. Dorsum of head gray-tan with distinct black speckles of varying size on the head shields; lateral surface of head with three bold, black vertical bars, one at the anterior margin of eye, one originating on the ventral eyelid and one just posterior to the orbit, all

Table 2. Morphological data for *Pedioplanis branchi* sp. nov. type specimens. CAS = California Academy of Sciences, MCZ = Museum of Comparative Zoology, ZMB = Museum für Naturkunde. Abbreviations for character values are as follows: C = In contact; S = Separated by granule; SF = Separated by frontal and frontonasal; RGN = Tail regenerated. See Materials and Methods for character abbreviations and descriptions.

Type Status	Holotype	Paratype	Paratype	Paratype	Paratype	Paratype	Paratype	Paratype
Museum No.	CAS 214788	ZMB89310	ZMB89311	CAS 214790	CAS 214792	CAS 214794	ZMB 89305	ZMB 89316
Sex	Male	Female	Female	Male	Male	Male	Male	Male
SVL (mm)	46.6	48	42.5	50.0	40.0	49.0	44.1	46.6
TaL (mm)	92.3	88.4	111.2	107.0	99.0	99.0	94.1	60.9 (RGN)
PF	C	SF	C	C	C	C	C	SF
G	8	12	14	11	11	14	11	9
RG	1	2	2	2	2	2	2	1
Su	6	5	6	6	6	7	7	6
IO	C	C	C	C	C	C	C	C
IF	7	6	6	7	6	6	7	6
Gu	30	30	26	30	26	30	32	28
SuL	26	29	28	26	25	25	27	29
Fe	11	10	12	12	10	13	13	11
PV	24	25	24	24	24	24	23	24

extending onto the supralabial scales; body dorsum uniform gray-tan with small, dense, indistinct black speckles. The flanks bear reticulate patterning and possess a single row of eight ocelli with light gray-blue spots of varying size (comprising 8–11 granules) bordered by indistinct black rings of 1–3 granules in width; black rings of adjacent ocelli either separated by 2–4 granules, or in some cases connected; venter cream; limbs pigmented above similar to dorsum, and white below; dorsum of tail with black speckling that is denser than that of the dorsum of body; tail transitions to pinkish-yellow towards the end; ventral surface of the tail is uniformly light cream.

Variation within the type series. Measurements for the type series are summarized in Table 2 and mensural (n = 20) and meristic (n = 33) character data based on measurements of additional museum vouchers can be found in Suppl. material 2, 3, respectively. Paratypes have similar scalation to holotype except: the prefrontals are separated by frontal and frontonasal in ZMB 89310 and ZMB 89316; the number of granules in group preceding the anterior supraocular varies from nine to 14; in ZMB 89316 there is only one row of granules dividing the supraoculars from the supraciliaries; in CAS 214794 and ZMB 89305 there are seven supraciliaries and five in ZMB 89310 on both sides of the head (usually six); there are usually 6 to 7 infralabials anterior to the subocular; gular scales in a straight line between symphysis of chin shields and median collar plate 26–32; subdigital lamellae under fourth toe 25–29; femoral pores 10–13 (RL only); presacral vertebrae 23–25.

Coloration in life (Fig. 8). Dorsal coloration and pattern varied considerably across examined specimens. Dorsum of head ranges from uniformly gray to distinctly speckled with black, sometimes with bold dark blotches or vertical bars. Body dorsum gray anteriorly and red-orange posteriorly, sometimes bearing light or dark spots that can be arranged in longitudinal rows, or are irregularly scattered, or may form horizontal bars or chevrons across the posterior dorsum near the tail base; belly uniform cream. The flanks may be patterned with light or dark irregular markings, sometimes forming vertical bars or chevrons, and are always lined with a more or less distinct longitudinal row of yellow spots or yellow-centered ocelli bordered by a broken ring of black granules, which range from 0.5–1.0 mm in diameter. The anterior surface of the thighs sometimes tinged with yellow; limbs and feet uniformly gray (front) or reddish–brown (hind), or speckled with light or black dots or blotches that may form bars. Dorsum of tail is orange–red, often with dense, black speckles.

Coloration (in alcohol). In comparison to the life coloration, the row of spots along the flanks that appear yellow in life appear gray-blue in preserved specimens and may be conspicuous or faint, and the reddish-brown color of the posterior body and tail appears darker and more grayish.

Distribution. *Pedioplanis branchi* sp. nov. is endemic to the Erongo Region in Namibia. Its range stretches from just south of the Swakop River in the South, where it occurs in parapatry with *P. husabensis*, through the pro-Namib, to the Ugab River and the Brandberg in the north and Mount Erongo and Otjimbingwe in the east, probably occurring in parapatry with *P. mayeri* all along its northeastern border (see Fig. 6 for map of locality records).

Etymology. The specific epithet is a patronym formed in the genitive singular honoring our friend and colleague, the British-born South African herpetologist, William Roy Branch (1946–2018), in recognition of his many contributions to African herpetology and in remembrance of many happy trips in the field together.

Natural history. *Pedioplanis branchi* inhabits Namibian savanna woodlands and the gravel plains and rocky outcrops in the Namib Desert (Deserts & Xeric Shrublands biome; Olson et al. 2001). The species is active on harder substrates, gravel and bare rock (including marble, granite, basalt), mostly with only sparse vegetation cover and only rarely forages on softer sandy substrates (e.g. in small washes on slopes) or in more grassy patches (Fig. 9). Median annual precipitation within the distribution range of *P. branchi* reaches a maximum of only 187 mm (minimum = 16 mm, median = 142 mm), while mean annual temperatures are similar to those in

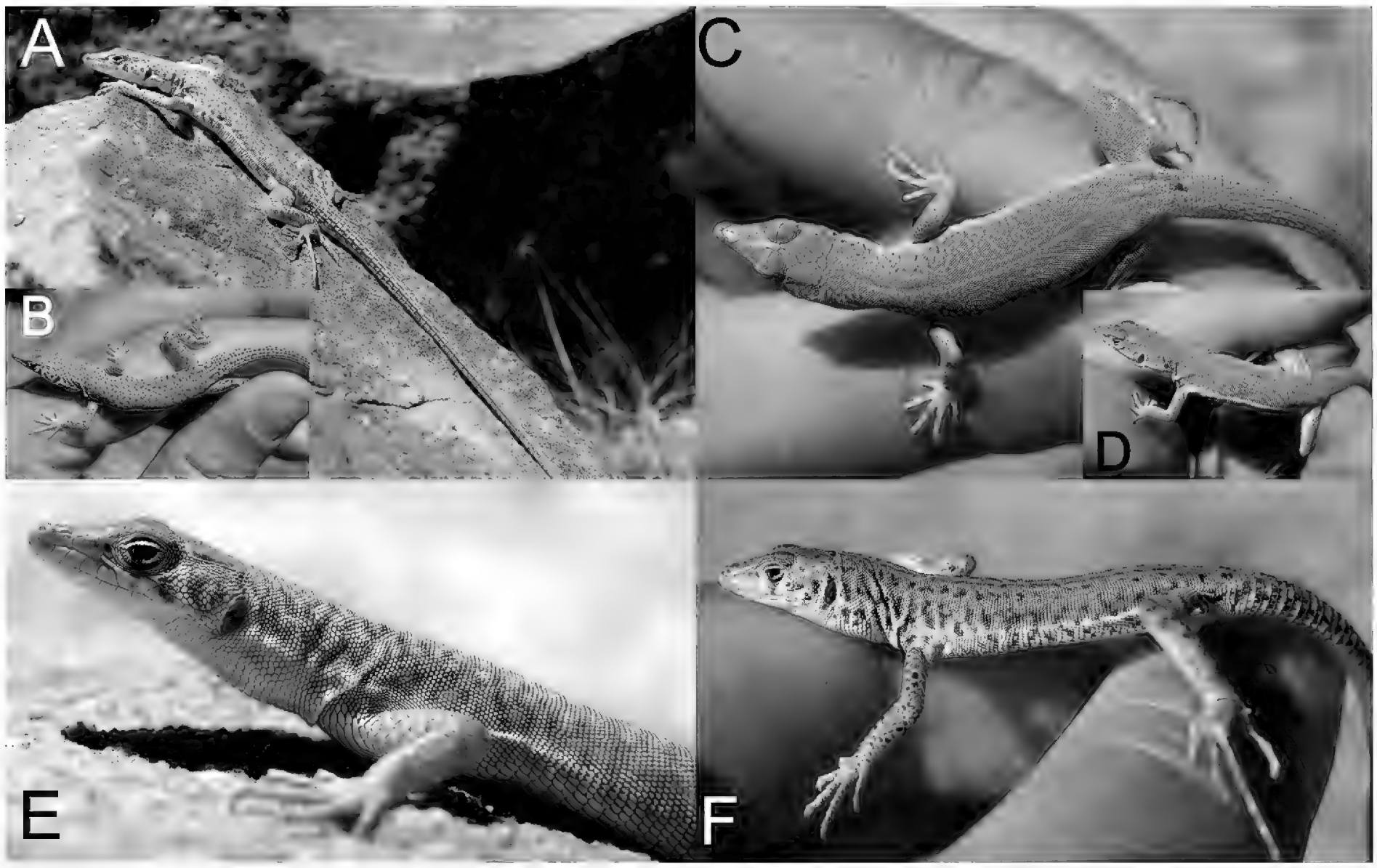

Figure 8. Life photographs of representative individuals of *Pedioplanis branchi* sp. nov. highlighting color pattern variation within the species. (**a.**) Lateral and (**b.**) dorsal whole body images of an adult specimen from the Chuos Mountains (Chuosberg) (SK376.2014; not included in study), note the dense, dark speckling on the dorsum, and bold dark lateral markings. (**c.**) Dorsal and (**d.**) lateral whole body images of an adult specimen (SK402.2014; not included in study) from the northward extension of the Swakop River Canyon, note the more uniformly gray and red dorsum lacking speckling and fainter yellow spots along the flanks. Lateral (**e.**) head and (**f.**) whole body images of an adult specimen from the northward extension of the Swakop River Canyon; note the black, vertical bar beneath the lower eyelid, the bold, dark lateral markings on the body, and the distinct longitudinal row of yellow spots along the flanks.

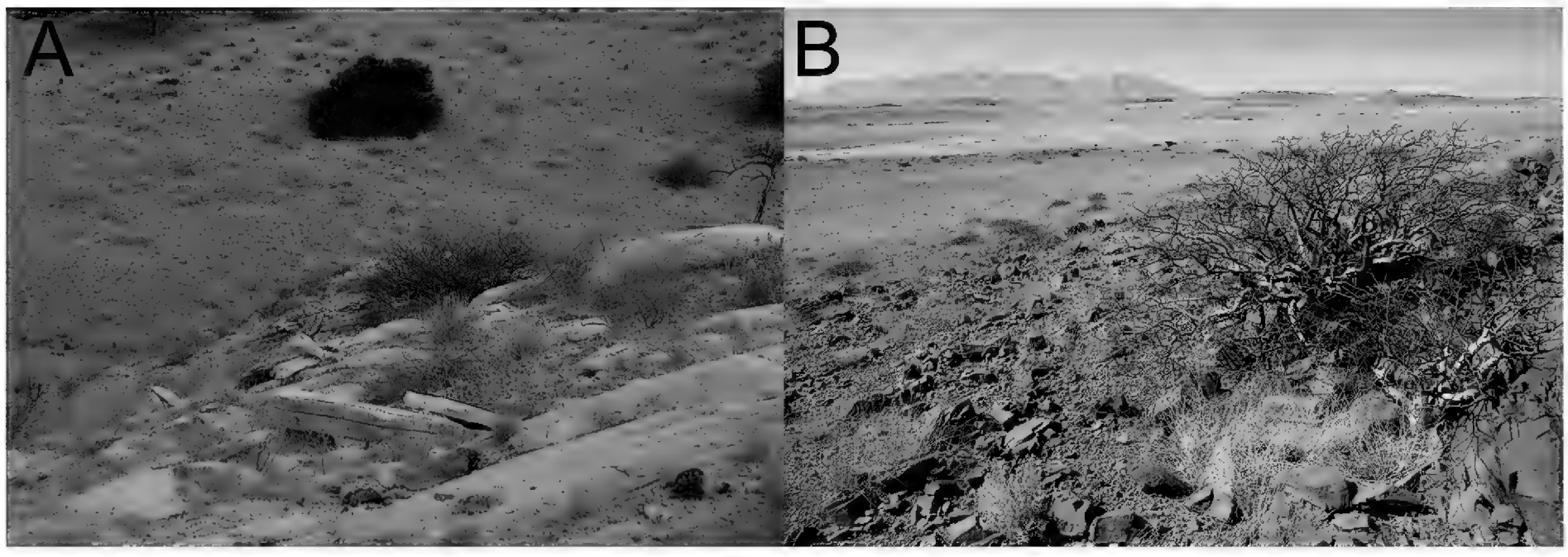

Figure 9. Habitat of *Pedioplanis branchi* sp. nov. (**a.**) Collection site for ZMB 89310 (Farm Friedhelm Sack, Erongo Region, Namibia) from the extended Swakop River Canyon on a marble/calc silicate slope with sparse grass cover and isolated shrubs. (**b.**) Collection site for ZMB 89612 (not included in study) from a small hill slope in the Tsiseb conservancy in the Pro-Namib, 20 km south of the Brandberg (visible in the background) depicting a sparsely vegetated scree slope with a *Commiphora* shrub.

the distribution of *P. mayeri* (median = 21 °C, range 19.4–22.5 °C). The species occupies lower elevations, from 77 m a.s.l. near the coast to a maximum of ca. 1190 m a.s.l. near the southeasternmost corner of the distribution along the Swakop River Canyon (median = 968 m a.s.l.). The largest recorded individual was a male (SVL = 50 mm). Breeding season appears to be similar to other southern African *Pedioplanis* spp. in spring, gravid females were found in December. Sympatric diurnal lizards include, *Trachylepis sulcata*, *Rhoptropus boultoni*, *Agama planiceps*, *Matobosaurus validus*, and *Varanus albigularis*, among others.

Conservation status. Although *P. branchi* has an extent of occurrence below 20,000 km^2 it occurs in an area with low human population density, generally low intensity land use, and a high proportion of suitable habitat. Populations occur in protected areas within Namib-Naukluft Park and Tsiseb Conservancy, and possibly Dorob National Park. Applying IUCN criteria we consider *P. branchi* to be Least Concern.

Discussion

Pedioplanis phylogeny and the recognition of two new species within the *P. undata* species complex

In order to resolve the systematics and biogeography of the *Pedioplanis undata* species complex we analyzed a new and greatly extended multi-locus molecular dataset comprising 455 samples, from all 13 currently recognized species of *Pedioplanis* and eight outgroup taxa. The results from our phylogenetic analyses show that interspecific relationships within the genus *Pedioplanis* are largely congruent with previous studies, but with several notable exceptions. We recover with strong support the phylogenetic affinities of three species that have heretofore remained problematic, *P. benguelensis*, *P. husabensis* and *P. rubens*. Within the *P. undata* species complex our results support the recognition of two highly divergent lineages and multiple instances of polyphyly.

Historically, *P. benguelensis* was thought to be closely related to *P. namaquensis* due to similarities in dorsal patterning (Bocage 1867; Laurent 1964; Makokha et al. 2007). More recently, Conradie et al. (2012) recovered *P. benguelensis* as sister to the Angolan species pair *P. huntleyi* + *P. haackei* and the *P. undata* complex, with *P. husabensis* falling outside of the entire grouping, however these results did not receive high nodal support in their analyses. Our results confirm the sister relationship between the Angolan taxa and members of the *P. undata* complex, however we recover *P. husabensis* and *P. benguelensis* as sequentially more distant sister taxa to this clade (Fig. 1b, c). Previous phylogenetic studies have obtained conflicting topologies for the placement of *P. rubens*. Maximum likelihood analyses by Makokha et al. (2007) found that *P. rubens* forms a clade with *P. undata* (actually, *P. mayeri* sp. nov.) that is sister to *P. gaerdesi* + *P. inornata*. However, their BI analysis recovered *P. rubens* as nested within the *P. undata* complex, a result corroborated by Conradie et al. (2012) and by this present study (Figs 1c, 2a).

We identify two instances of polyphyly within the *P. undata* complex. First, *P. inornata* as previously defined comprises two divergent lineages, one that occurs in the eastern and southern parts of Namibia, and in the Northern Cape of South Africa (= *P. inornata*) and another comprising individuals from central-western Namibia (= *P. branchi* sp. nov.). The two lineages are not each other's closest relatives; rather, *P. branchi* sp. nov. is sister to *P. gaerdesi*. This result was corroborated by the nuclear data, in which the concatenated phylogeny recovered these clades as being distinct from one another. Interestingly, some *P. branchi* sp. nov. individuals possess a single (instead of two) large semi-transparent scale ("brille") in the lower eyelid, which caused them to be identified as *P. gaerdesi* in the field given that this scale character is currently used to diagnose the species (Conradie et al. 2012). We suggest that this morphological character alone is inadequate for diagnosing species within the *P. undata* complex. Makokha et al. (2007) identified the presence of a *P. inornata* "Central" clade (= *P. branchi* sp. nov.), however, due to limited sampling they were unable to identify its geographic extent. Here we provide evidence that this clade is limited to an arid region north of the Kuiseb River and south of the Ugab River. These results corroborate Mayer and Berger-Dell'mour's (1987) hypothesis that within *P. inornata* there exist two geographically and morphologically distinct forms, one restricted to west-central Namibia that possesses a gray forebody and red-orange hindbody with yellow lateral spots (*P. inornata*-"Central" = *P. branchi* sp. nov.; body coloration depicted in Fig. 8), and a more broadly distributed form in southern Namibia that is characterized by brownish or reddish coloration with greenish lateral spots, *P. inornata*-"South" (= *P. inornata*).

Another equally striking result is the discovery that *P. undata* comprises two genetically distinct and polyphyletic lineages. The first clade, *P. undata* "North" (= *P. mayeri* sp. nov.) includes individuals primarily from northern Namibia, (although a single sample was found as far south as Nauchas), and is sister to all remaining members of the *P. undata* species complex. The second lineage, *P. undata* "South" (= *P. undata* sensu stricto), is more deeply nested within the complex and is closely related to *P. inornata*, a result recovered by both the nuclear and mtDNA data.

Diversification and geographic context

Geographic isolation of populations through vicariance can result from various events, including both geological (formation of rivers, valleys, mountains, dunes) and climatic (drastic environmental change resulting from cooling, warming, or changes in precipitation resulting in habitat expansion or contraction). Southern Africa has experienced a complex paleoclimatic and geological past. In particular, the climatic oscillations of the Upper Miocene and the Pliocene-Pleistocene era are proposed to have been influential in the evolution and diversification of southern African fauna (e.g. Bauer 1999; Matthee and Flemming 2002; Montgelard and Matthee 2012).

In addition, multiple potential geographical barriers have been hypothesized to be responsible for vicariance and subsequent cladogenesis. These include the Great Escarpment, the sand seas of the Namib Desert, shifting Kalahari sands, and rivers such as the Kuiseb, Zambezi,

and Orange (e.g. Lamb and Bauer 2000; Matthee and Flemming 2002; Scott et al. 2004; Bauer et al. 2006).

The current distribution ranges of members of the *P. undata* complex (see Fig. 6) do not indicate that the aforementioned barriers today have a substantial effect in restricting gene flow. For example, the sister taxa *P. inornata* and *P. undata* both occur east and west of the escarpment and instead possess a north-south border (*P. undata* also occurs both north and south of the Kuiseb), and the sister pair *P. branchi* and *P. gaerdesi* both occur west of the escarpment with a north-south border not obviously coincident with any geographical barrier. Nevertheless, during the estimated times of major cladogenesis events within the genus (ca. 8–3.8 million years ago (MYA); Makokha et al. 2007; Garcia-Porta et al. 2019) these potential physical barriers of gene flow may have been less porous and only later, in concert with the Plio-Pleistocene/Holocene climatic changes, may have permitted passage.

During the Early Miocene conditions in southern Africa were wetter and warmer than today. Since then southern Africa has undergone stepwise cooling and drying. Diekmann et al. (2003) suggested that arid periods occurred in southern Africa between 11.6 and 10.7 MYA and between 9.7 and 7.7 MYA. The region experienced a third major cooling step with increased aridification at the end of the Pliocene (around 2.8 MYA) (Van Zinderen Bakker 1986; Partridge 1998; Diekmann 2003). This coincided with a major uplifting of the subcontinent (the African superswell; Lithgow-Bertelloni and Silver 1998) resulting in major changes of erosional patterns due to rejuvenation and reactivation of drainage systems and increased fluvial activity (Partridge et al. 2006). These drastic climatic changes may have resulted in newly available open habitats for *Pedioplanis* species occupying more arid habitats like *P. branchi*, facilitating subsequent radiation and then likely led to range contractions and fragmentation among ancestral *Pedioplanis* spp. with subsequent cladogenesis, scenarios that have been suggested for e.g. southern African *Pachydactylus* geckos (Bauer 1999; Heinicke et al. 2017) and lacertids generally (Garcia-Porta et al. 2019).

The major uplift together with changes in drainage systems during less arid periods at the end of the Pliocene seems to coincide well with the split of *P. inornata* and *P. undata*, indicating that the now ephemeral Kuiseb and/or Swakop River might have been effective impediments to gene flow between these two sister taxa in the past. Today, in the east there are populations of *P. undata* occurring south of the mostly dry Kuiseb, indicating that gene flow between the two taxa is possible. For *P. mayeri* (the basal taxon of the clade) and *P. gaerdesi*, the escarpment has been suggested to form a geographical barrier (Bauer et al. 1993). During our study we detected a narrow area of potential sympatry north of Palmwag and – based on museum specimens – near Sesfontein, suggesting that while the escarpment might have formed a barrier in the past it no longer does.

Evolution of body coloration and patterning within the *P. undata* species complex

The *P. undata* species complex has historically proven taxonomically challenging, in part due to the fact that most species have been distinguished chiefly by their body coloration and patterning (Branch 1998; Conradie et al. 2012). Our phylogenetic results show both that divergent taxa share similar color and patterning characteristics, and that intraspecific variation can be considerable.

Dorsal striping may be a plesiomorphic condition within the *P. undata* complex given that *P. mayeri*, the sister taxon to the remainder of the complex, as well as the Angolan outgroup species *P. huntleyi* and *P. haackei*, are all typically striped. The absence of dorsal striping in *P. rubens*, *P. inornata* and *P. gaerdesi* would suggest that stripes were lost in lineages that subsequently invaded more open habitats (further discussed below) whereas the ancestral, striped condition was retained within *P. undata*.

Members of the *P. undata* species complex are chiefly allopatrically distributed in regions of Namibia that are ecologically distinct; we suggest that apparent color variation both among and within species may be a result of differences in habitat and associated selective pressures. Uniformly and plainly colored taxa including *P. branchi*, *P. gaerdesi*, *P. inornata* and *P. rubens* all occur in arid regions where they are camouflaged on bare, sandy or rocky substrates that lack dense vegetation (Arino et al. 2012; Stone and Thomas 2013). In the case of *P. rubens*, which has a very restricted range in the Waterberg Plateau, individuals are reddish and are found exclusively on red sandstone, whereas *P. gaerdesi* and *P. branchi* are found in similar habitats in the pro-Namib and adjacent rocky outcrops of the Namib, respectively, and each possesses a light gray dorsum, especially anteriorly. Likewise, striped patterning in *P. mayeri* and northern populations of *P. undata* may also be a consequence of shared similarities in habitat type. Both taxa occur in inland localities in northern Namibia, a region that receives 200–500 mm of rainfall annually (Rohde and Hoffman 2012) and in habitats predominantly characterized by annual and perennial grasses (Arino et al. 2012; Wang et al. 2012). Among squamates the correlation between dorsal striping and the use of grassy substrates has been hypothesized to reflect the use of disruptive coloration in order to reduce the likelihood of detection by predators during escape (Wolf and Werner 1994; Farallo and Forstner 2012).

This hypothesized link between ecology and body coloration in the *P. undata* species complex may be further demonstrated by the pronounced intraspecific variation evident within the sister taxa *P. inornata* and *P. undata*. For example, within *P. inornata*, typical specimens possess a predominantly gray dorsum, however we encountered localized red morphs on red, hard-packed soils ca. 60 km west of Mariental, and dark morphs on basalt rock piles just north of the same town. *Pedioplanis undata* collected in northern localities that are characterized by substantial grass cover (Harris et al. 2014) exhibit bold dorsal stripes

that appear nearly indistinguishable from those exhibited by *P. mayeri* (see Fig. 4 for images of dorsal color patterning typical of the species), whereas individuals collected just south of the Khomas Hochland, where grasses are more sparsely distributed, possess faint gray dorsal stripes; furthermore, individuals collected near the Gobabeb Training and Research Centre on vegetationless, schist rock outcrops had almost patternless, nearly uniformly gray dorsums.

Taken together, our phylogenetic results and field observations strongly suggest that ecology is a significant evolutionary driver of body coloration and patterning within the *P. undata* species complex, as has also been demonstrated previously for e.g. *P. lineoocellata* (Branch 1998; Edwards 2013; Childers 2015).

Conclusion

The results of our study indicate that species diversity within Namibian *Pedioplanis* is greater than previously thought and that this diversity is concentrated within the *P. undata* species complex. These results settle the long-standing hypothesis originally put forth by Mayer and Berger-Dell'mour (1987) on the existence of additional lineages within the complex and confirm that it comprises six species rather than the four traditionally considered.

Based on present species distributions and divergence date estimates derived from previous phylogenetic studies on African lacertids (Makokha et al. 2007; Garcia-Porta et al. 2019 we propose several biogeographic scenarios that may have led to cladogenesis in the *P. undata* species complex. We hypothesize that species diversification beginning at ca. 8–3.8 MYA may have been precipitated by major climatic changes in combination with the formation of biogeographic barriers across the subcontinent, causing once widespread populations to become isolated and restricting gene flow until cladogenesis ultimately ensued. Among these isolated populations, differences in habitat and associated natural selection pressures may have produced phenotypic differences among them including the evident diversity in body color and patterning between species.

This study highlights the need for dense geographic sampling among broadly distributed groups that have radiated recently and rapidly, as is the case for the genus *Pedioplanis*. Furthermore, without fine-scaled microhabitat data it is difficult to accurately assess ecological differences and to test our hypothesis of convergent evolution in this group, and we recommend future researchers prioritize these critical data.

The majority of organismal research in Namibia has so far mainly focused on the Namib Desert region in the west (Herrmann and Branch 2013), where species discovery has accelerated over the past decade due in part to the implementation of molecular phylogenetics. However, this study highlights the need for increased biodiversity surveys of the central interior portion of Namibia, as our results suggest that squamate endemicity in this region may have been previously underestimated.

Acknowledgements

We thank the permit issuing authorities in Angola, South Africa and Namibia for allowing the collection of specimens within their respective jurisdictions. Curators and collections managers of the institutions cited in Tables 1 and 2 and Suppl. material 1 are thanked for their generous access to specimens and provision of tissue samples and data. We are especially grateful to Carol Spencer (MVZ), Lauren Scheinberg (CAS), José Rosado (MCZ), Frank Tillack and Mark-Oliver Rödel (MfN) for their assistance with specimen loans and access to collection facilities. Luke and Ursula Verburgt, Johan Marais, Mathew Heinicke, William Branch, Tomas Kleinert, Johannes Penner, Rodrigo Megía Palma, Laura Zamorano, Ammon Corl, Donald Miles, Lee Fitzgerald, Christy Hipsley and H. Berger-Dell'mour provided essential field assistance. Thank you, Kristin Mahlow and Johannes Müller (both MfN), for micro-CT scans of the ZMB specimens and logistic support. Thank you to Elisa Yang and Tomo Yoshino (both MVZ) for assistance with GenBank data accessioning. AMB was supported by NSF grant EF1241885, subaward 13–0632. SK was supported by the German Academic Exchange Service (DAAD) and the Elsa-Neumann-Stipendium des Landes Berlin (Humboldt University of Berlin, Germany).

References

Anonymous (2002) Opinion 1992 (Case 3085) *Lacerta undata* A. Smith, 1838 (currently *Pedioplanis undata*; Reptilia; Sauria): specific name conserved by the designation of a neotype. Bulletin of Zoological Nomenclature 59: e60.

Arino O, Perez JJR, Kalogirou V, Bontemps S, Defourny P, Van Bogaert E (2012) Global land cover map for 2009 (GlobCover 2009). European Space Agency and Université Catholique de Louvain, PANGAEA. https://doi.org/10.1594/PANGAEA.787668

Arnold EN (1991) Relationships of the South African lizards assigned to *Aporosaura*, *Meroles* and *Pedioplanis* (Reptilia: Lacertidae). Journal of Natural History (25): 783–807. https://doi.org/10.1080/00222939100770511

Arnold EN, Arribas O, Carranza S (2007) Systematics of the Palaearctic and Oriental lizard tribe Lacertini (Squamata: Lacertidae: Lacertinae), with descriptions of eight new genera. Zootaxa 1430(1): 1–86. https://doi.org/10.11646/zootaxa.1430.1.1

Bauer AM (1999) Evolutionary scenarios in the *Pachydactylus* group geckos of southern Africa: new hypotheses. African Journal of Herpetology 48(1–2): 53–62. https://doi.org/10.1080/21564574.1999.9651072

Bauer AM, Branch WR, Haacke WD (1993) The herpetofauna of the Kamanjab area and adjacent Damaraland, Namibia. Madoqua 18(2): 117–145.

Bauer AM, Shea G (2006) *Pedioplanis inornata* (Roux, 1907); Plain Sand Lizard; maximum size. African Herp News 40: 1–19.

Bauer AM, Lamb T, Branch WR (2006) A revision of the *Pachydactylus serval* and *P. weberi* groups (Reptilia: Gekkota: Gekkonidae) of Southern Africa, with the description of eight new species. Proceedings of the California Academy of Sciences 57(23): 595–709.

Berger-Dell'mour HA, Mayer W (1989) On the parapatric existence of two species of the *Pedioplanis undata* group (Reptilia: Sauria: Lacertidae) in the central Namib Desert (Southwest Africa) with description of the new species *Pedioplanis husabensis*. Herpetozoa 1: 83–95.

Bocage JVB du (1867) Segunda lista dos répteis das possessões portuguezas d'África ocidental que existem no Museu de Lisboa. Jornal de Ciências, Matemáticas, Físicas e Naturais de Lisboa 3: 217–228.

Boulenger GA (1921) Monograph of the Lacertidae (Vol. II). Trustees of the British Museum of Natural History, London, 451 pp. https://doi.org/10.5962/bhl.title.8312

Borsuk-Bialynicka M, Lubka M, Böhme W (1999) A lizard from Baltic amber (Eocene) and the ancestry of the crown group lacertids. Acta Palaeontologica Polonica 44: 349–382.

Branch WR (1998) Field guide to snakes and other reptiles of southern Africa (3rd edn.). Ralph Curtis Books Publishing, Sanibel Island, 399 pp.

Childers JL (2015) Phylogenetics and phylogeography of southern African sand lizards, *Pedioplanis* (Sauria:Lacertidae). MSc thesis, Villanova University. Villanova, Pennsylvania.

Conradie W, Measey GJ, Branch WR, Tolley KA (2012) Revised phylogeny of African sand lizards (*Pedioplanis*), with the description of two new species from south-western Angola. African Journal of Herpetology 61: 91–112. https://doi.org/10.1080/21564574.2012.676079

Cunningham M, Cherry MI (2004) Molecular systematics of African 20-chromosome toads (Anura: Bufonidae). Molecular Phylogenetics and Evolution 32: 671–685. https://doi.org/10.1016/j.ympev.2004.03.003

Daan S, Hillenius D (1966) Catalogue of the type specimens of amphibians and reptiles in the Zoological Museum, Amsterdam. Beaufortia 13: 117–144.

de Queiroz K (1998) The general lineage concept of species, species criteria, and the process of speciation. In: Howard SJ, Berlocher SH (Eds) Endless Forms: Species and Speciation. Oxford University Press, New York, 57–58.

Diekmann B, Fälker M, Kuhn G (2003) Environmental history of the south-eastern South Atlantic since the Middle Miocene: Evidence from the sedimentological records of ODP Sites 1088 and 1092. Sedimentology 50(3): 511–529. https://doi.org/10.1046/j.1365-3091.2003.00562.x

Duméril AMC, Bibron G (1839) Erpétologie Générale ou Histoire Naturelle Compléte Des Reptiles. Tome Cinquième. Contenant l'histoire de quatre-vingt-trois genres et deux cent sept espèces des trois dernieres familles de l'ordre des sauriens, savoir: Les lacertiens, les chalcidiens et les sincoïdiens. Paris, Libraire Encyclopédique de Roret, [viii +] 854 [+ 1] pp. [4 folding tables, pls. 37, 39, 39bis, 41bis, 49, 51–54, 56–58]

Edgar RC (2004) MUSCLE: multiple sequence alignment with high accuracy and high throughput. Nucleic Acids Research 32(5): 1792–1797. https://doi.org/10.1093/nar/gkh340

Edwards S (2013) Patterns and processes of adaptation in lacertid lizards to environments in southern Africa. PhD thesis, Stellenbosch University. Matieland, South Africa.

Engleder A, Haring E, Kirchhof S, Mayer W (2013) Multiple nuclear and mitochondrial DNA sequences provide new insights into the phylogeny of South African lacertids (Lacertidae, Eremiadinae). Journal of Zoological Systematics and Evolutionary Research 51: 132–143. https://doi.org/10.1111/jzs.12012

Farallo VR, Forstner MR (2012) Predation and the maintenance of color polymorphism in a habitat specialist squamate. PLoS ONE 7: e30316. https://doi.org/10.1371/journal.pone.0030316

Fick SE, Hijmans RJ (2017) WorldClim 2: new 1-km spatial resolution climate surfaces for global land areas. International Journal of Climatology 37: 4302–4315. https://doi.org/10.1002/joc.5086

Fox J, Weisberg S (2019) An R companion to applied regression (3rd edn.). Sage, Thousand Oaks, CA. https://socialsciences.mcmaster.ca/jfox/Books/Companion/

Garcia-Porta J, Irisarri I, Kirchner M, Rodríguez A, Kirchhof S, Brown JL, MacLeod A, Turner AP, Ahmadzadeh F, Albaladejo G, Crnobrnja-Isailovic J, de la Riva I, Fawzi A, Galán P, Göçmen B, Harris DJ, Jiménez-Robles O, Joger U, Jovanović Glavaš O, Karış M, Koziel G, Künzel S, Lyra M, Miles DB, Nogales Hidalgo MJ, Anıl Oğuz M, Pafilis P, Rancilhac L, Rodríguez N, Rodríguez Concepción B, Sanchez E, Salvi D, Slimani T, S'khifa A, Qashqaei AT, Žagar A, Lemmon A, Moriarty Lemmon E, Carretero MA, Carranza S, Philippe H, Sinervo B, Müller J, Vences M, Wollenberg Valero KC (2019) Environmental temperatures shape thermal physiology as well as diversification and genome-wide substitution rates in lizards. Nature Communications 10: 1–12. https://doi.org/10.1038/s41467-019-11943-x

Harris A, Carr AS, Dash J (2014) Remote sensing of vegetation cover dynamics and resilience across southern Africa. International Journal of Applied Earth Observation and Geoinformation 28: 131–139. https://doi.org/10.1016/j.jag.2013.11.014

Heinicke MP, Jackman TR, Bauer AM (2017) The measure of success: geographic isolation promotes diversification in *Pachydactylus* geckos. BMC Evolutionary Biology 17(1): e9. https://doi.org/10.1186/s12862-016-0846-2

Herrmann HW, Branch WR (2013) Fifty years of herpetological research in the Namib Desert and Namibia with an updated and annotated species checklist. Journal of Arid Environments 93: 94–115. https://doi.org/10.1016/j.jaridenv.2012.05.003

Hipsley CA, Müller J (2017) Developmental dynamics of ecomorphological convergence in a transcontinental lizard radiation. Evolution 71(4): 936–948. https://doi.org/10.1111/evo.13186

Kirchhof S, Hipsley CA, Corl A, Dell'mour H, Müller J (2014) Geographical distributions. *Pedioplanis undata* (Smith, 1838) Western Sand Lizard. African Herp News 61: 30–33.

Kirchhof S, Hetem RS, Lease HM, Miles DB, Mitchell D, Müller J, Rödel MO, Sinervo B, Wassenaar T, Murray IW (2017) Thermoregulatory behavior and high thermal preference buffer impact of climate change in a Namib Desert lizard. Ecosphere 8: e02033. https://doi.org/10.1002/ecs2.2033

Lamb T, Bauer AM (2000) Relationships of the *Pachydactylus rugosus* group of geckos (Reptilia: Squamata: Gekkonidae). African Zoology 35(1): 55–67. https://doi.org/10.1080/15627020.2000.11407192

Lanfear R, Frandsen PB, Wright AM, Senfeld T, Calcott B (2016) PartitionFinder2: new methods for selecting partitioned models of evolution for molecular and morphological phylogenetic analyses. Molecular Biology and Evolution 34(3): 772–773. https://doi.org/10.1093/molbev/msw260

Laurent RF (1964) Reptiles et amphibiens de l'Angola (Troisème contribution). Publicações Culturais. Companhia de Diamantes de Angola 67: 1–165.

Lithgow-Bertelloni C, Silver PG (1998) Dynamic topography, plate driving forces and the African superswell. Nature 395(6699): 269–272. https://doi.org/10.1038/26212

Makokha JS, Bauer AM, Mayer W, Matthee CA (2007) Nuclear and mtDNA-based phylogeny of southern African sand lizards, *Pedioplanis* (Sauria: Lacertidae). Molecular Phylogenetics and Evolution 44: 622–633. https://doi.org/10.1016/j.ympev.2007.04.021

Matthee CA, Flemming AF (2002) Population fragmentation in the southern rock agama, *Agama atra*: more evidence for vicariance in Southern Africa. Molecular Ecology 11(3): 465–471. https://doi.org/10.1046/j.0962-1083.2001.01458.x

Mayer W, Berger-Dell'mour HAE (1987) The *Pedioplanis undata* complex (Sauria, Lacertidae) in Namibia. A system of parapatric species and subspecies. In: Gelder V, Strijbosch JJ, Bergers PJM (Eds) Proceedings of the 4th Ordinary General Meeting of the Societas Europaea Herpetologica, Nijmegen, 275–278.

Mayer W, Böhme W (2000) Case 3085. *Lacerta undata* A. Smith, 1838 (currently *Pedioplanis undata*; Reptilia; Sauria): proposed conservation of the specific name by the designation of a neotype. Bulletin of Zoological Nomenclature 57: 100–102. https://doi.org/10.5962/bhl.part.20689

Mayer W, Pavlicev M (2007) The phylogeny of the family Lacertidae (Reptilia) based on nuclear DNA sequences: convergent adaptations to arid habitats within the subfamily Eremiainae. Molecular Phylogenetics and Evolution 44: 1155–1163. https://doi.org/10.1016/j.ympev.2007.05.015

Mertens R (1954) Neue Eidechsen aus Südwest-Afrika. Senckenbergiana Biologica 34: 175–186.

Mertens R (1955) Die Amphibien und Reptilien Südwestafrikas aus den Ergebnissen einer im Jahre 1952 ausgeführten Reise. Abhandlungen der Senckenbergischen Naturforschenden Gesellschaft 490: 1–172.

Miller M, Pfeiffer W, Schwartz T (2010) Creating the CIPRES Science Gateway for inference of large phylogenetic trees. In: Proceedings of the Gateway Computing Environments Workshop (GCE). IEEE, New Orleans, Louisiana, 1–8. https://doi.org/10.1109/GCE.2010.5676129

Olson DM, Dinerstein E, Wikramanayake ED, Burgess ND, Powell GVN, Underwood EC, D'Amico JA, Itoua I, Strand HE, Morrison JC, Loucks CJ, Allnutt TF, Ricketts TH, Kura Y, Lamoreux JF, Wettengel WW, Hedao P, Kassem KR (2001) Terrestrial ecoregions of the world: a new map of life on Earth. Bioscience 51(11): 933–938. https://doi.org/10.1641/0006-3568(2001)051[0933:TEOTWA]2.0.CO;2

Montgelard C, Matthee CA (2012) The GDRI 191 (2007–2010): Biodiversity and global change in southern Africa. Acta Oecologica 42: 1–2. https://doi.org/10.1016/j.actao.2012.05.012

Partridge TC (1998) Of diamonds, dinosaurs and diastrophism: 150 million years of landscape evolution in southern Africa. South African Journal of Geology 101(3): 167–184.

Pavlicev M, Mayer W (2009) Fast radiation of the subfamily Lacertinae (Reptilia: Lacertidae): History or methodical artefact? Molecular Phylogenetics and Evolution 52: 727–734. https://doi.org/10.1016/j.ympev.2009.04.020

QGIS.org (2021) QGIS Geographic Information System. QGIS Association. http://www.qgis.org

R Core Team (2019) R: A language and environment for statistical computing. R Foundation for Statistical Computing. Vienna. https://www.R-project.org/

Rambaut A, Drummond AJ, Xie D, Baele G, Suchard MA (2018) Posterior summarization in Bayesian phylogenetics using Tracer 1.7. Systematic Biology 67(5): 901–904. https://doi.org/10.1093/sysbio/syy032

Rohde RF, Hoffman MT (2012) The historical ecology of Namibian rangelands: vegetation change since 1876 in response to local and global drivers. Science of the Total Environment 416: 276–288. https://doi.org/10.1016/j.scitotenv.2011.10.067

Rohland N, Reich D (2012) Cost-effective, high-throughput DNA sequencing libraries for multiplexed target capture. Genome Research 22: 939–946. https://doi.org/10.1101/gr.128124.111

Ronquist F, Huelsenbeck JP (2003) MrBayes 3: Bayesian phylogenetic inference under mixed models. Bioinformatics 19: 1572–1574. https://doi.org/10.1093/bioinformatics/btg180

Roux J (1907) Beiträge zur Kenntnis der Fauna von Süd-Afrika. VII. Lacertilia (Eidechsen). Zoologische Jahrbücher, Abteilung für Systematik, Geographie und Biologie der Tiere 25: 403–444. [pls. 14–15] https://doi.org/10.5962/bhl.part.11960

Scott IAW, Keogh JS, Whiting MJ (2004) Shifting sands and shifty lizards: molecular phylogeny and biogeography of African flat lizards (*Platysaurus*). Molecular Phylogenetics and Evolution 31: 618–629. https://doi.org/10.1016/j.ympev.2003.08.010

Stamatakis A (2014) RAxML version 8: a tool for phylogenetic analysis and post-analysis of large phylogenies. Bioinformatics 30: 1312–1313. https://doi.org/10.1093/bioinformatics/btu033

Stone AEC, Thomas DSG (2013) Casting new light on late Quaternary environmental and palaeohydrological change in the Namib Desert: A review of the application of optically stimulated luminescence in the region. Journal of Arid Environments 93: 40–58. https://doi.org/10.1016/j.jaridenv.2012.01.009

Van Zinderen Bakker EM, Mercer JH (1986) Major late Cainozoic climatic events and palaeoenvironmental changes in Africa viewed in a world wide context. Palaeogeography, Palaeoclimatology, Palaeoecology 56(3–4): 217–235. https://doi.org/10.1016/0031-0182(86)90095-7

Wang L, Katjiua M, D'Odorico P, Okin GS (2012) The interactive nutrient and water effects on vegetation biomass at two African savanna sites with different mean annual precipitation. African Journal of Ecology 50: 446–454. https://doi.org/10.1111/j.1365-2028.2012.01339.x

Wickham H (2016) ggplot2: elegant graphics for data analysis. Springer-Verlag New York. ISBN 978-3-319-24277-4. https://ggplot2.tidyverse.org

Wickham H, François R, Henry L, Müller K (2021) dplyr: A grammar of data manipulation. R package version 1.0.4. https://CRAN.R-project.org/package=dplyr

Wolf M, Werner YL (1994) The striped colour pattern and striped/non-striped polymorphism in snakes (Reptile: Ophidia). Biological Reviews 69: 599–610. https://doi.org/10.1111/j.1469-185X.1994.tb01250.x

Appendix 1

Voucher specimens used for morphological analyses.

CAS = California Academy of Sciences, MCZ = Museum of Comparative Zoology, ZMB = Museum für Naturkunde. Specimens in bold were not sequenced; X-rayed or CT scanned specimens are denoted with § superscript (micro-CT scans available on the MfN Data Repository, DOI: 10.7479/4jg6-ae46; X-ray images available on MorphoSource.com, DOI: 10.17602/M2/M350312, M350317, M350322, M350327, M35036, M350352, M350362, M350367, M350372, M350377, M350384, M350391, M350396, M350401, M350406, M350411, M350416,

M350421, M350427, M350432, M350437, M350442). Type specimens are denoted with asterisks (** = holotype; * = paratype). All raw data is available upon request from the corresponding author (JLC).

Pedioplanis branchi sp. nov. – **CAS 126221§**, **173423§**, **173442§**, **173445§**, **173446**, 214787§, 214788§**, 214789, **214790§***, 214792§*, 214793§, **214794§***; MCZ-R184162§ (x-ray only); ZMB 89302, 89303, 89304, 89305§*, 89306, 89307, 89308, 89309, 89310§*, 89311§*, 89312, 89313, 89314, 89315, 89316§*, 89317, 89318, 89319, 89320, 89321, **89613**.

Pedioplanis gaerdesi – CAS 206964, 214599, 214729, **214730**, **214741**, **214742**, **214743**, **214744**, 214745, 214746; MCZ-R184294, 184959, 185875, 185883, 185885, 185887, 185888, 188237; ZMB 89328, 89329, 89330, 89331, 89332, **89612**.

Pedioplanis inornata – CAS 193404, 200012, 200039, **200096**, 201873, 203522; MCZ-R183772, 184767, 185890, 193103, 193104, 193105, 193293, 193311, 193370; ZMB 89333, 89334, 89336, 89337, 89338, 89339, 89340, 89341.

Pedioplanis mayeri sp. nov. – CAS 214643§*, **214644§**, **214645§***, 224010§, 224013; MCZ-R185870§*, 185872§*, 188223§, 190213§*, 193125§*, 193178§, 193179§**; ZMB 80391, 89349§*, 89350§*, **89624**, **89625**.

Pedioplanis rubens – ZMB 84748, 89351, **89615**, **89616**, **89617**, **89618**, **89619**, **89620**, **89621**, **89622**, **89623**.

Pedioplanis undata – MCZ-R188247, 188248, 193272, 193276, 193376; **ZMB 91631, 89626**, **89627**, **89628**, **89629**, **89630**, **89631**.

Supplementary material 1

Sampling list for all specimens used in phylogenetic analyses

Authors: Jackie L. Childers, Sebastian Kirchhof, Aaron M. Bauer

Data type: excel table

Explanation note: Locality information and GenBank accession numbers are provided for all tissue vouchers used in this study. We also provide the specimen ID numbers and mtDNA clade assignments for members of the *Pedioplanis undata* species complex that are depicted in Fig. 2a, b. Institutional abbreviations for catalog numbers are as follows: CAS = California Academy of Sciences, MCZ = Museum of Comparative Zoology, NHMW = Naturhistorisches Museum Wien, PEM = Bayworld (Port Elizabeth, SA), ZMB = Museum für Naturkunde. Collector and associated field number abbreviations are as follows: ABA-ABD-ABE = Werner Mayer, AMB = Aaron M. Bauer, JM = Johan Marais, JVV = Jens V. Vindum, KTH = Krystal Tolley, MB-MBUR = Marius Burger, MH = Michael Cunningham, N = Anamarija Zagar, RBH = Raymond B. Huey, SK = Sebastian Kirchhof, SVV = Stuart V. Nielson, USH = University of Stellenbosch Herpetology, WC = Werner Conradie. AMB, MCZ-A, and MCZ-Z specimens lacking institutional registration numbers are currently awaiting cataloging at the National Museum of Namibia.

Link: https://doi.org/10.3897/zse.97.61351.suppl1

Supplementary material 2

Mensural data for *P. undata* species complex specimens examined.

Authors: Jackie L. Childers, Sebastian Kirchhof, Aaron M. Bauer

Data type: excel table

Explanation note: Minimum and maximum values (mm) for each species are reported for each character, see Materials and methods for character abbreviations and descriptions. Only adults were examined, and only individuals with intact tails were used to obtain tail length values (TaL); see Appendix 1 for a list of all specimens examined.

Link: https://doi.org/10.3897/zse.97.61351.suppl2

Supplementary material 3

Meristic and scalation data for *P. undata* species complex specimens examined.

Authors: Jackie L. Childers, Sebastian Kirchhof, Aaron M. Bauer

Data type: excel table

Explanation note: Abbreviations for character values are as follows: C = In Contact; S = Separated by granule; SF = Separated by frontal and frontonasal; SP = Separated by parietals. Data were collected from juvenile and adult specimens. See Materials and methods for character abbreviations and descriptions; see Appendix 1 for a list of all specimens examined.

Link: https://doi.org/10.3897/zse.97.61351.suppl3

Supplementary material 4

Table S1. Primer pairs

Authors: Jackie L. Childers, Sebastian Kirchhof, Aaron M. Bauer
Data type: excel table
Explanation note: Primers pairs used in this study; PCR annealing temperatures (°C) are provided.

Link: https://doi.org/10.3897/zse.97.61351.suppl4

Supplementary material 5

Table S2. Bayesian partitioning schemes

Author: Jackie L. Childers
Data type: excel table
Explanation note: Bayesian partitioning schemes for the concatenated mtDNA (Partition nos. 1–4) and concatenated nDNA (Partition nos. 5–8) datasets based on the results of our PartitionFinder v.2.1.1 analyses, in which best-fitting models of evolution were selected using the Bayesian Information Criterion (BIC) score.

Link: https://doi.org/10.3897/zse.97.61351.suppl5

Supplementary material 6

Table S3. Summary statistics for select meristic variables for *P. undata* species complex

Author: Sebastian Kirchhof
Data type: excel table
Explanation note: Summarized results of Shapiro-Wilk normality test, Levene's test, Kruskal-Wallis rank sum test and ANOVA for selected meristic variables for adults (SVL $\geq$ 40 mm) of all species of the *P. undata* species complex. Columns show character (see Materials and Methods for abbreviations and descriptions), Shapiro-Wilk W (Shapiro_W) and corresponding p-value (Shapiro_p), Levene's F (Levene_F) and corresponding p-value (Levene_p), Kruskal-Wallis chi-square statistics (KW_chi-squared) and corresponding p-value (KW_p), ANOVA F (ANOVA_F) and corresponding p-value (ANOVA_p) and degrees of freedom (df). Differences are considered significant with $p \leq 0.05$ and significance codes are as follows: * = $p < 0.5$; ** = $p < 0.01$; *** = $p < 0.001$.

Link: https://doi.org/10.3897/zse.97.61351.suppl6

Supplementary material 7

Table S4. Summarized results of Wilcoxon rank sum tests for the meristic characters

Author: Sebastian Kirchhof
Data type: excel table
Explanation note: Summarized results of Wilcoxon rank sum tests for the meristic characters with significant Kruskal-Wallis test results (number of subdigital lamellae SuL and number of femoral pores on right leg Fe). All possible species pairs (species pair) for species of the *P. undata* species complex were tested. Columns show Wilcoxon W (Wilcox_W) and corresponding p-value (Wilcox_p) and significant differences ($p \leq 0.05$) are indicated with * and significance codes are as follows: * = $p < 0.5$; ** = $p < 0.01$; *** = $p < 0.001$.

Link: https://doi.org/10.3897/zse.97.61351.suppl7

Supplementary material 8

Figure S1. Linear relationships with 95% confidence level intervals of mensural characters between *P. mayeri* (= *P. undata* "North") and *P. undata*

Author: Sebastian Kirchhof
Data type: PNG image
Explanation note: Linear relationships with 95% confidence level intervals of mensural characters with snout–vent length (SVL) for adult (SVL ≥ 40 mm) *P. mayeri* (= *P. undata* "North" sensu Mayer and Berger-Dell'mour 1987) and *P. undata*. Linear regression equations are provided when the slope coefficient was significant ($p \leq 0.05$), in case of non-significance this is indicated by "not sig." abbreviations; descriptions of characters are provided in Materials and methods.

Link: https://doi.org/10.3897/zse.97.61351.suppl8

Supplementary material 9

Figure S2. Linear relationships with 95% confidence level intervals of mensural characters between *P. branchi* (= *P. inornata* "Central") and *P. inornata*

Author: Sebastian Kirchhof
Data type: PNG image
Explanation note: Linear relationships with 95% confidence level intervals of mensural characters with snout–vent length (SVL) for adult (SVL ≥ 40 mm) *P. branchi* (= *P. inornata* "Central" sensu Makokha et al. 2007) and *P. inornata*. Linear regression equations are provided when the slope coefficient was significant ($p \leq 0.05$), in case of non-significance this is indicated with "not sig." abbreviations; descriptions of characters are provided in Materials and methods.

Link: https://doi.org/10.3897/zse.97.61351.suppl9